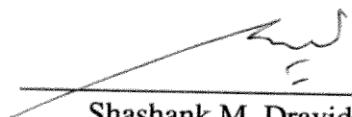



THESIS APPROVED BY

08/05/2015

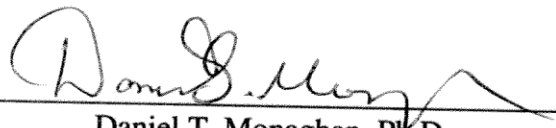
Date



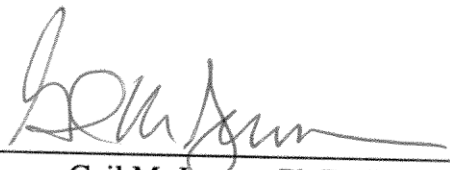
Shashank M. Dravid, Ph.D., Chair



Timothy M. Simeone, Ph.D.



Daniel T. Monaghan, Ph.D.



Gail M. Jensen, Ph.D., Dean

Identification of novel gating mechanisms underlying pharmacological potentiation of NMDA receptors

By

DIVYAN A. CHOPRA

A Master's thesis by

Submitted to the faculty of the Graduate School of the Creighton University
in Partial Fulfillment of the Requirements for the degree of Master of
Science in the Department of Pharmaceutical Sciences.

Omaha, NE

(month, day, and year)

ABSTRACT

Excitatory neurotransmission mediated by N-methyl-D-aspartate receptors (NMDARs) is known to play an important role in synaptic plasticity, learning and memory. Moreover, NMDAR dysfunction may contribute to a variety of neuropsychiatric and neurological disorders including schizophrenia, epilepsy, stroke and trauma. Pregnenolone sulfate (PS) is one of the most commonly occurring neurosteroids in the central nervous system and influences function of several receptors. PS modulates NMDARs and has been shown to have both positive and negative modulatory effects on NMDAR currents generally in a subtype-selective manner. We assessed the gating mechanism of PS modulation of GluN1/GluN2A receptors transiently expressed in HEK 293 cells using whole-cell and single-channel electrophysiology. Only a modest effect on the whole-cell responses was observed by PS in dialyzed (non-perforated) whole-cell recordings. Interestingly, in perforated conditions, PS was found to increase the whole-cell currents in the absence of nominal extracellular Ca^{2+} whereas PS produced an inhibition of the current responses in the presence of 0.5 mM extracellular Ca^{2+} . The Ca^{2+} -binding DRPEER motif and GluN1 exon-5 were found to be critical for the Ca^{2+} -dependent bidirectional effect of PS. Single-channel cell-attached analysis demonstrated that PS primarily affected the mean open time to produce its effects, with positive modulation mediated by an increase in duration of open time constants while negative modulation mediated by a reduction in the time spent in a long-lived open state of the receptor. Further kinetic modeling of the single-channel data suggested that the positive and negative modulatory effects are mediated by different gating steps which may represent GluN2 and GluN1 subunit-selective conformational changes respectively. Our studies provide a unique mechanism of

modulation of NMDARs by an endogenous neurosteroid which has implications for identifying state-dependent molecules. UBP (University of Bristol Pharmaceuticals) series compounds act at allosteric binding sites on the NMDARs and have been able to achieve subtype-selectivity. We found that UBP684 significantly increased the whole-cell current and mean open time and reduced the mean shut time for GluN1/GluN2A receptors. Mutagenesis studies suggest that UBP684 can stabilize the closed cleft of the LBD and drive the receptor into the more stable open states.

PREFACE

Publications:

Chopra, D. A., Monaghan, D. T., & Dravid, S. M. (2015). Bidirectional Effect of Pregnenolone Sulfate on GluN1/GluN2A NMDA Receptor Gating Depending on Extracellular Calcium and Intracellular Milieu. *Molecular Pharmacology*.
<http://doi.org/10.1124/mol.115.100396>

Chopra, D.A., Irvine, M.W., Jane, D.E., Monaghan, D. T., & Dravid, S. M. (In preparation). Gating Effects of a Novel Allosteric Modulator at GluN1/GluN2A NMDA Receptors.

Ka, M., Jung, E M., Chopra, D. A., Dravid, S. M., Kim, W. Y. (Submitted to JNS). Essential roles for ARID1B in dendritic arborization and spine formation of developing pyramidal neurons

ACKNOWLEDGEMENTS

This work would have not been possible without the help and support of my advisor and mentor Dr. Shashank M. Dravid. I would really like to thank him for his constant support and encouragement and his readiness to help and train me and get the best out of me. I have enjoyed discussing scientific concepts, talking about new research ideas, and troubleshooting when I was stuck in a problem. I have also enjoyed playing a few games of soccer and squash with him from time to time. I also would like to thank my committee members Dr. Daniel T. Monaghan and Timothy M. Simeone for their valuable inputs and feedback and constant encouragement during the MS program. I am thankful to my lab members Dr. Subhash Gupta, Ratnamala Pavuluri, Dr. Roopali Yadav, Aparna Ravikrishnan and Jinxu Liu for teaching me various techniques and their help and guidance throughout.

I would want to thank my friends Aisha, Pratik, Rishabh, Amruta, Pushkar, Akash, and our entire Kellom Group for caring and helping like a family.

I express my gratitude towards the Almighty to have made all this possible.

DEDICATION

I would like to dedicate this thesis to my parents Usha Chopra and Ashok Chopra for their continuous help, support, caring and encouragement. I would also like to dedicate this to my grandparents and my family members for their support throughout.

TABLE OF CONTENTS

	Page No
Abstract	iii
Preface	v
Acknowledgements	vi
Dedication	vii
Table of contents	Viii
List of figures	Xi
List of tables	Xiii
Chapter 1: Introduction	1
A. Expression and trafficking of NMDARs	3
B. Structure and activation of NMDARs	4
C. Kinetic and biophysical properties of NMDARs	7
D. Role of NMDARs in physiology and disease	8
E. Drugs acting at NMDARs	10
E1. Channel blockers	10
E2. Orthosteric agents	11

E3. Allosteric modulators	12
E4. Advantages of allosteric modulators	13
F. Pregnenolone sulfate	15
G. Kinetic modeling for NMDARS	17
Chapter 2: Bidirectional effect of pregnenolone sulfate on GluN1/GluN2A NMDA receptor gating depending on extracellular calcium and intracellular milieu	20
A. Abstract	21
B. Introduction	22
C. Materials and methods	23
D. Data processing and kinetic modeling	25
E. Results	26
F. Discussion	33
G. Figures	39
H. Tables	46
I. References	48
Chapter 3: Stabilization of closed glutamate-binding domain as a gating mechanism of a novel GluN1/GluN2A receptor potentiator	66
A. Abstract	67
B. Introduction	68
C. Materials and methods	69
D. Data processing and kinetic modeling	71
E. Results	72

F. Discussion	75
G. References	85

LIST OF FIGURES

Chapter 1		
Figure 1:	Classification of glutamate receptors based on their pharmacology and structural homology.	2
Figure 2:	Expression patterns of different GluN2 subunits in postnatal and adult mouse brain	4
Figure 3:	Membrane topology of an ionotropic glutamate receptor subunit depicting the ATD, LBD, TMD and intracellular CTD domains	4
Figure 4:	Influence of GluN2 subunit composition on NMDAR deactivation kinetics	7
Figure 5:	Different binding sites for agonists, antagonists and modulators are shown for NMDARs	9
Figure 6:	Strategies for NMDAR drug development over the past few years and potentially useful classes of drugs	15
Figure 7:	Chemical structure of pregnenolone sulfate	15
Figure 8:	Physical model of NMDA receptor activation as proposed by Banke and Traynelis.	17
Figure 9:	Cyclic model for NMDAR activation as proposed by Zhou and Auerbach	18
Chapter 2		
Figure 1:	Modulation of whole-cell responses by pregnenolone sulfate is dependent on intracellular milieu and extracellular calcium	39
Figure 2:	Molecular determinants of inhibition by pregnenolone sulfate in the presence of external Ca ²	40

Figure 3:	Pregnenolone sulfate increases open probability of GluN1/GluN2A receptors.	41
Figure 4:	Pregnenolone sulfate mediated potentiation of GluN1/GluN2A receptors involves a shift in open states to longer durations and a reduction in the occupancy of long-lived shut states	42
Figure 5:	Pregnenolone sulfate mediated potentiation of GluN1/GluN2A receptors involves a shift in open states to longer durations and a reduction in the occupancy of long-lived shut states	43
Figure 6:	Inhibitory effect of pregnenolone sulfate on GluN1/GluN2A receptors is primarily due to reduced dwell-time in a longer open state	44
Figure 7:	Kinetic mechanism describing the effects of pregnenolone sulfate on GluN1/GluN2A receptor activation	45
Chapter 3		
Figure 1:	Modulation of whole-cell responses by UBP684 is dependent on mode of recording	80
Figure 2:	UBP684 mediated potentiation of GluN1/GluN2A receptors involves a shift in open states to longer durations and a reduction in the occupancy of long-lived shut states.	81
Figure 3:	Effect of UBP684 and NR1c/NR2A ^c mutant on shut-time parameters	82
Figure 4:	Cysteine modifications in the LBD for obtained locked agonist binding clefts	83
Figure 5:	Docking images which show the site of binding of UBP684 at GluN1/GluN2A receptors	84

LIST OF TABLES

Table 1:	Time constants and areas of closed and open components obtained from exponential fits.	46
Table 2:	Hidden Markov maximum interval likelihood fitting of the steady state currents.	47
Table 3:	Time constants and areas of closed and open components obtained from exponential fits.	78
Table 4:	Hidden Markov maximum interval likelihood fitting of the steady state currents.	79

Chapter 1

Introduction

Introduction

Glutamate is a major neurotransmitter in the central nervous system (CNS) mediating excitatory neurotransmission in the brain and when released pre-synaptically, it activates a variety of glutamate receptors. Iontropic glutamate receptors mediate the excitatory synaptic transmission in the central nervous system and are localized in neuronal and non-neuronal cells. Iontropic glutamate receptors are grouped into four distinct categories based on their pharmacology and structural homology, namely NMDA receptors (GluN1, GluN2A–GluN2D, GluN3A, and GluN3B), the AMPA receptors (GluA1–GluA4), the kainate receptors (GluK1–GluK5), and the delta receptors (GluD1 and GluD2) (Traynelis et al., 2010).

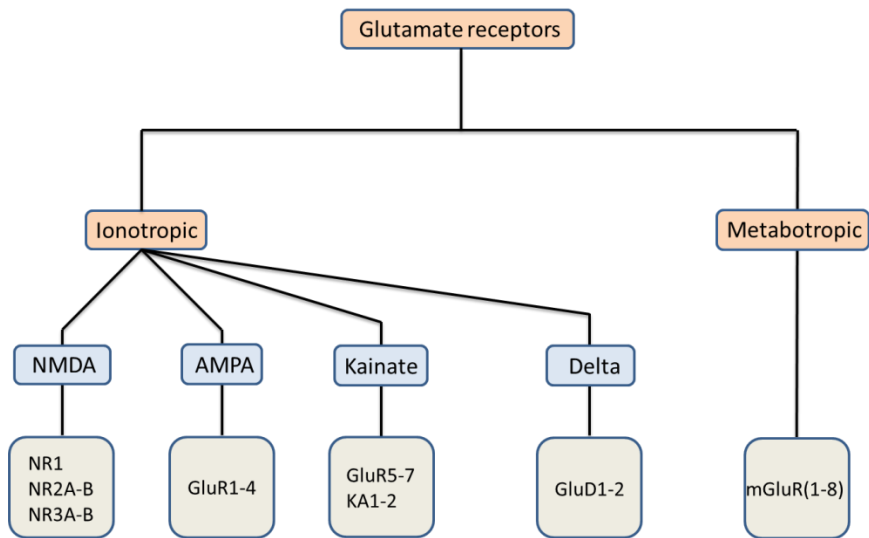


Figure 1: Classification of glutamate receptors based on their pharmacology and structural homology.

A. Expression and trafficking of NMDARs

Synaptically, NMDARs are mostly co-localized along with AMPA receptors which is essential for synaptic plasticity and long term potentiation (Collingridge et al., 2004). There are certain synapses, which only contain AMPA receptors and they are known as silent synapses (Kerchner and Nicoll, 2008). The GluN1 subunit is widely expressed in the cortex and hippocampus in the fetal brain, but it becomes more widespread as development progresses (Moriyoshi et al., 1991). The GluN2A subunit expression starts shortly after birth and is highly expressed in the forebrain in regions of hippocampus, cerebral cortex, thalamus and in the cerebellum (Paoletti et al., 2013). The GluN2B subunit is mostly developmental and is restricted to just the forebrain as development proceeds (Paoletti et al., 2013., Cull-Candy et al., 2001). The GluN2C subunit is mostly expressed in the cerebellum and olfactory bulb, while the GluN2D subunit shows mostly fetal expression in the caudal regions (Cull-Candy et al., 2001; Moriyoshi et al., 1991). However, as development progresses the expression is drastically reduced and in the adult brain it is just expressed in the diencephalon and mesencephalon (Paoletti et al., 2013., Paoletti, 2011). An interesting concept about the expression of NMDARs is the presence of an endoplasmic reticulum (ER) retention signal. The masking of these signals occurs after the formation of a functional receptor, after which they exit the ER and are delivered to the synapse. The GluN1 subunit is vital for the release of GluN2 subunits from the ER (Lau and Zukin., 2007).

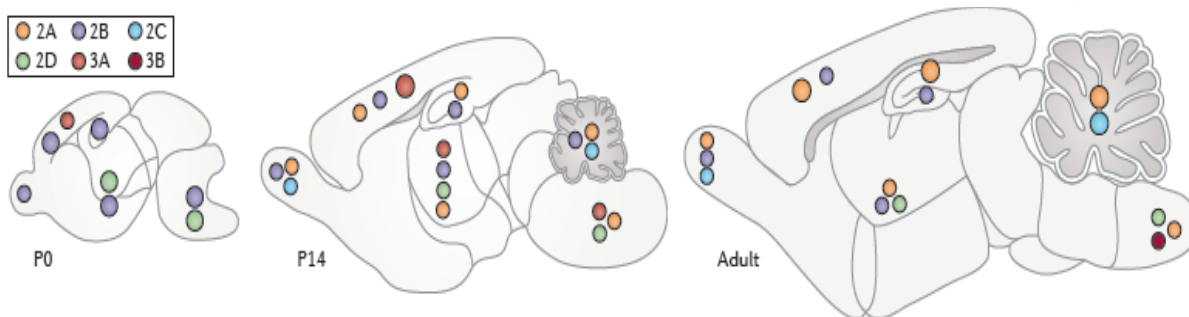


Figure 2: Expression patterns of different GluN2 subunits in postnatal and adult mouse brain (Paoletti and Zhou, 2013).

B. Structure and activation of NMDARs

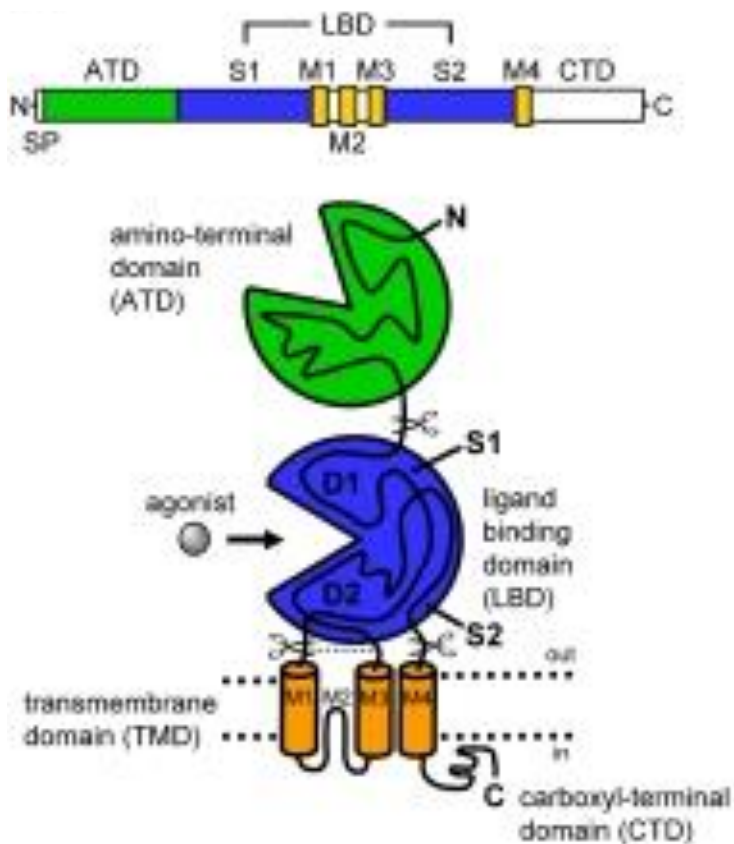


Figure 3: Membrane topology of an ionotropic glutamate receptor subunit depicting the ATD, LBD, TMD and intracellular CTD domains (Traynelis et al., 2010).

NMDA receptors (NMDARs) are one of the major ionotropic glutamate receptors at central synapses (Traynelis et al., 2012). NMDARs are tetrameric receptors typically composed of two glycine-binding GluN1 subunits and two glutamate-binding GluN2 subunits (A-D) (Traynelis et al., 2010). In addition to glycine, D-serine and D-alanine may also serve as endogenous ligands for GluN1 subunit (Pullan et al., 1987). Unlike AMPA and kainite receptors, NMDARs are obligate heterotetramers and exhibit a 1-2-1-2 subunit arrangement pattern (Behe et al., 1995; Sobolevsky et al., 2009). There are as many as eight splice variants of the GluN1 subunit. The GluN1-1b splice variant is characterized by the presence of exon-5 which has been found to regulate several biophysical and pharmacological characteristics of the receptor. (Moriyoshi et al., 1991; Blahos and Wenthold., 1996; Chaffrey et al., 2008). The GluN2A and GluN2B subunits share 70% sequence homology while GluN2C and GluN2D subunits share about 55% homology (Monyer et al., 2012).

Each subunit consists of an amino terminal domain (ATD), the ligand binding domain (LBD), the transmembrane domain (TMD) and the intracellular carboxyl-terminal domain (CTD). The TMD is made up of M1, M3, M4 transmembrane segments and M2, a re-entrant loop, (Traynelis et al., 2010). The ATD domain of the NMDAR has a similar clamshell-like conformation like the LBD (Karakas et al., 2009). Truncation of the ATD does not affect the receptor assembly and trafficking, however, it has an influence on open probability, desensitization and deactivation of the receptors (Meddows et al., 2001; Gielen

et al., 2009; Yuan et al., 2009; Traynelis et al., 2010). The CTD is thought to influence membrane targeting, post-translational modifications and phosphorylation-dephosphorylation pathways of the receptors (Traynelis et al., 2010). The CTD is the least conserved domain among all the NMDAR subtypes (Ryan et al., 2008).

The LBD domain of the NMDAR adopts a clamshell-like conformation. The segment S1, located on the amino-terminal position of membrane helix M1, forms most of one half of the clamshell (D1), and the segment S2 between the M3 and M4 membrane helices forms most of the opposite half of the clamshell (D2). The agonist binding pocket is placed inside the crevice between these two lobes. Activation of NMDARs involves three steps: The first step involves binding of an agonist at the LBD (Traynelis et al., 2010). The second step involves a conformational change in the clamshell of the LBD (Armstrong and Gouaux, 2000). The third step involves a conformational change in the ion-channel that is connected to the LBD (Zhang et al., 2008). During agonist application, the agonist binds non-covalently to the receptors, facilitating the transition of the receptors from open-cleft to closed-cleft conformation, which further entraps the agonist (Abele et al., 2000; Cheng et al., 2005). This receptor-ligand interaction involves an initial rapid “association”, followed by slower conformational changes known as “docking” and then stabilization of the complex known as “locking” (Abele et al., 2000). This locked conformation is quasi-stable and can go from closed to active or desensitized conformations (Wollmuth and Sobolevsky, 2004). It is assumed that the M3 segment in the transmembrane domain plays a key role in the gating of NMDARs. This has been shown by examining the effects of a point mutation in the SYTANLAAF region of the M3 segment (known as the Lurcher mutation), leading to constitutively open channels (Zuo et al., 1997; Traynelis et al., 2010).

C. Kinetic and biophysical properties of NMDARs

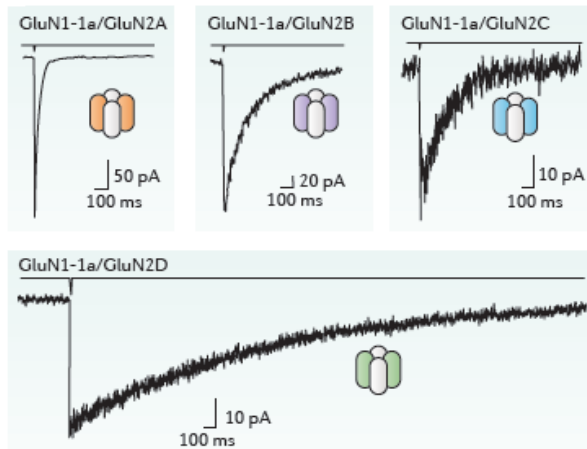


Figure 4: Influence of GluN2 subunit composition on NMDAR deactivation kinetics (Paoletti and Zhou, 2013)

NMDARs have a large and uniform single-channel conductance and slower gating kinetics and deactivation time course as compared to AMPA and kainite receptors (Erreger et al., 2005, Monyer et al., 1992). Kainite receptors have slower current than AMPA receptors (Castillo et al., 1997). AMPA and kainite receptors show fast desensitization and a considerable reduction in steady state currents. However, NMDARs show slower desensitization and comparatively lower inhibition of steady state current. The different subtypes of NMDARs have diverse biophysical, biochemical and pharmacological properties (Traynelis et al., 2010, Paoletti, 2011). Among the NMDAR subtypes, GluN2A shows slower desensitization as compared to GluN2B receptors, and GluN2C and GluN2D show little or no desensitization (Banke et al., 2005; Traynelis et al., 2010). GluN2A receptors show faster deactivation kinetics as compared to the other subtypes. The deactivation is slow for GluN2B and GluN2C subunits, while and GluN2D subunit shows

the slowest deactivation (Paoletti et al., 2013). NMDA receptor subtypes also differ in their maximal open probability. They range from about 0.5 for GluN2A, to 0.01 for GluN2C and GluN2D subtypes (Chen et al., 1999).

NMDARs are highly permeable to calcium, however, they also have some Ca^{2+} binding sites on them. The binding of calcium to these sites causes a reduction in single channel conductance (Gibb and Colquhoun, 1991; Premkumar and Auerbach, 1996). One of the external calcium binding site is situated in the DRPEER motif which is located C-terminus to the M3 transmembrane segment in the GluN1 subunit (Sharma and Stevens, 1996; Watanabe et al., 2002; Traynelis et al., 2010). This DRPEER motif, however is absent in GluN2 subunit, AMPA, kainate and delta receptors (Watanabe et al., 2002). Another Ca^{2+} binding site is located in the ion-channel pore known as the QRN site (Jahr and Stevens, 1993). All NMDARs exhibit a magnesium block at -70mV, which is relieved on depolarization beyond -40mV.

D. Role of NMDARs in physiology and disease

NMDARs are important to the formation of memory, learning, and changes in synaptic strength and connectivity (Bliss et al., 1993; Hardingham and Bading, 2003). They also promote survival of neurons, maintain synaptic strength and connectivity. NMDAR potentiation is useful in treating cognitive disorders. It has also been shown that overexpression of GluN1/GluN2B receptors improves memory and learning ability in mice (Tang et al., 1999). The function of NMDARs in schizophrenia is essential, as seen by administering NMDA receptor blockers like PCP, which cause schizophrenia like effects (Tsai and Coyle, 2002). Potentiation of NMDARs might be therapeutically useful in

disorders like anxiety, cognitive impairment and post-traumatic stress disorder (Davis et al., 2006; Hofmann et al., 2006; Collingridge et al., 2012). On the contrary, over-excitation of NMDARs leads to neuronal death (Lipton and Rosenberg, 1994). Excessive potentiation of NMDARs can result in cerebral ischemia and stroke. In these conditions the dying neurons release excessive glutamate, which causes over activation of other neurons and this further leads to glutamate induced excitotoxicity (Kemp and Mckernan, 2002). Over-activation of NMDARs leads to neurodegenerative disorders like Alzheimer's disease and Parkinson's disease. In these disorders, neuronal damage causes an excessive release of glutamate to compensate for the reduced activity (Paoletti et al., 2013; Kalia et al., 2008; Schmitt et al., 2007; Hallett and Standaert., 2004).

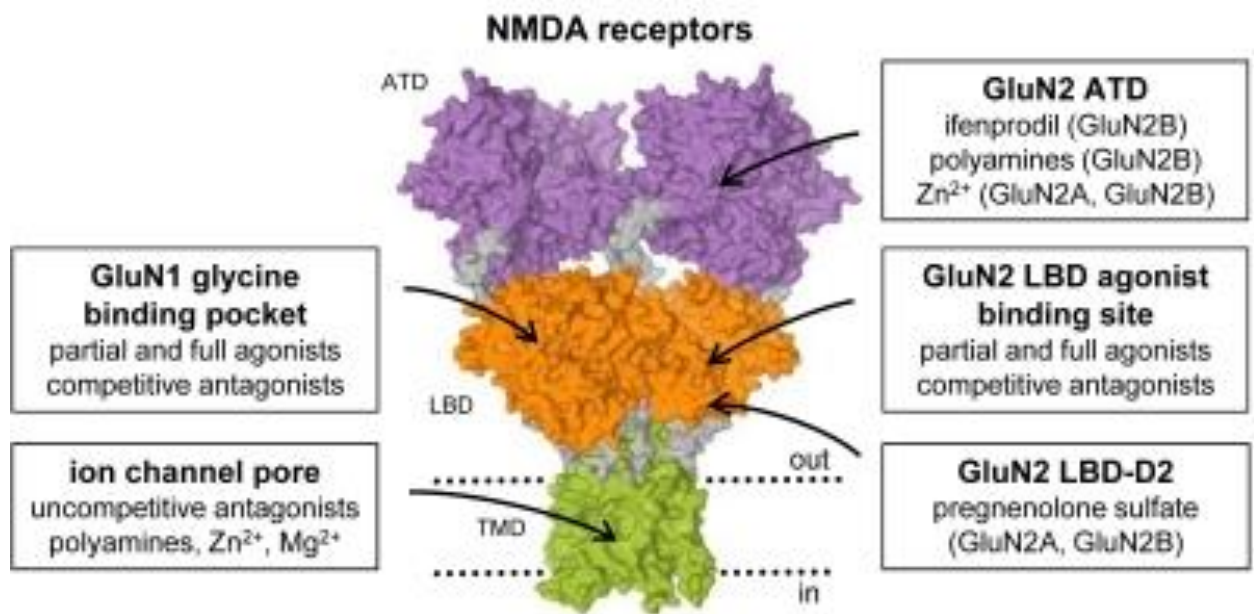


Figure 5: Different binding sites for agonists, antagonists and modulators are shown for NMDARs (Traynelis et al., 2010)

E. DRUGS ACTING AT NMDARs

It might appear that targeting NMDARs would open a huge therapeutic potential for the treatment of various disorders of the CNS. The discovery of compounds acting at NMDARs started around 25-30 years ago, however, they could not be used therapeutically. Clinical trials have failed due to low efficacy and tolerance issues with the drugs along with their non-selective action at NMDARs and occurrence of various side effects (Ikonomidou and Turski, 2002; Hoyte et al., 2004; Muir., 2006; Doppenberg et al 2004)., A need to develop agents for selective modulation of NMDARs is essential and new potential drugs are being explored for their actions at NMDARs via different mechanisms. The following section describes the different mechanisms and major binding sites which have been targeted for drug development.

The different compounds acting at the NMDARs can be classified as follows based on their mechanism and site of action:

E.1. NMDAR Channel blockers

NMDA channel pore blockers are uncompetitive antagonists and their action requires prior opening of the receptor. . These compounds can dissociate from the ion-channel only after reactivation of the receptor by agonists (Parsons et al., 1995; Blanpied et al., 1997; Traynelis et al., 2010). Compounds like MK-801, ketamine and PCP are examples of high affinity channel blockers. Some channel blockers unbind rapidly as compared to the above mentioned compounds. They are recognized as partial blockers and an instance of this class is memantine (Chen and Lipton., 1997; Mealing et al., 1999). They work in a different manner as compared to other uncompetitive channel blockers since they have a lower binding affinity and faster dissociation kinetics (Chen and Lipton, 2006;

Kotermanski et al., 2009; Traynelis et al., 2010). These trapping blockers might be stabilizing the closed state of the receptor and promoting channel closure (Yuan et al., 2005). The synthetic compound MK-801 has higher affinity toward blocking GluN2A and GluN2B subtypes. However, the difference in selectivity is not large enough that it can be used to achieve subtype-selectivity (Paoletti and Neyton, 2007). One of the clinically used NMDARs channel blocker is memantine for Alzheimer's disease (Tariot, 2006; Winblad et al., 2007; Mobius and Stoffler, 2003). Memantine prefers to block the over activated and aberrant receptors, while sparing the normally functioning ones (Chen and Lipton., 2006). Another NMDAR ion-channel blocker, which has been approved for use in humans as an anesthetic agent is ketamine, belonging to the class of partially trapping uncompetitive channel blockers like memantine (Annetta et al., 2005; Hedegaard et al., 2012). Memantine and ketamine also show some anti-depressant properties, which has led to targeting NMDARs for the treatment of depression as well (Skolnick et al., 2009). Similar low affinity blockers like amantadine have shown promising results pre-clinically as an adjunct therapy to L-DOPA to treat Parkinson's disease, however it could not translate into clinical setting (Addy et al, 2009; Crosby et al., 2003).

E.2. NMDAR orthosteric agents

Orthosteric compounds are the ones which exert their effects by binding to the glutamate and glycine binding sites. The drugs acting at the glutamate binding site did not prove to be effective in clinical trials. A major reason for this is they cause complete activation of the receptor and do not provide the ability to fine tune the receptor response. They also have to compete with the endogenous neurotransmitter like glutamate which

shows a high affinity for NMDAR activation and this would require administration of a really high dose in order to achieve therapeutic efficacy (Kemp and Mckernan. 2002). This could further lead to non-specific side effects like hallucinations, disruption of cognition and psychotomimetic side effects. The highly conserved structure of the glutamate binding site, makes it difficult to target different subtypes using compounds acting at the glutamate binding site (Furukawa et al., 2005).

Glycine site partial agonists like D-serine are being studied extensively, as they have shown promising results in the treatment of schizophrenia and cognitive disorders (Heresco-Levy et al., 2002; Kemp and Mckernan., 2002). Studies have also been focused on increasing the synaptic D-serine concentration by inhibiting the enzyme serine racemase (Wolosker et al., 1991). Since the GluN1 subunit is present in all subtypes, they do not show subtype-selectivity (Furukawa et al., 2005),.

E.3. NMDAR allosteric modulators

Allosteric modulators are compounds which can bind to regulatory sites on the receptor other than the orthosteric binding sites (Paoletti, 2011; Traynelis et al., 2010). Zinc, an endogenously occurring ligand is an allosteric modulator, as it acts by binding to the ATD of the NMDARs. It has shown selectivity to the GluN2A subunit and acts as a negative allosteric modulator by reducing the mean duration and probability of opening of the channel. Discovery of ifenprodil, acting at the GluN1/GluN2B ATD interface and being 200-400 times more selective for GluN2B and GluN2A subunits respectively has drawn attention towards targeting the ATD for the development of highly selective compounds (Choi and Lipton., 1999; Traynelis et al., 1998; Karakas et al., 2011). Ifenprodil is found

to increase the inhibition of GluN1/GluN2B receptors, as the pH reduces. This property could be useful in conditions like ischemia, where the milieu turns acidic due to accumulation of glutamic acid (Bhatt et al., 2013). Protons inhibit NMDARs, however, they do so in a voltage independent manner (Banke et al., 2005). They inhibit GluN1/GluN2A receptors by reducing mean open time and open probability (Dravid et al., 2007). Neurosteroids are another class of interesting allosteric compounds which act on NMDARs. The potentiation by neurosteroids is subtype dependent. Pregnenolone sulfate, an endogenous neurosteroid potentiates GluN2A and GluN2B NMDARs, however has a lower efficacy at GluN2C and GluN2D receptors (Horak et al., 2006). UBP compounds are a series of naphthalene and phenanthrene derivatives which show promising effects on NMDARs and exhibit subtype-selectivity. (Monaghan et al., 2010). They may act as lead compounds in the development of more specific compounds in the future. Another compound acting allosterically at GluN2C and GluN2D receptors and gaining importance for future studies is CIQ (Mullaseril et al., 2010) as many positive allosteric modulators are not available.

E.4. Advantages of allosteric modulators

Allosteric modulators for NMDARs are still in the discovery stage, however, they have turned out to be very effective for GABA and G-protein coupled receptor signaling (Santangelo et al., 2012; Bowery et al., 2002; Langmead and Christopoulos, 2006). Allosteric modulators modify existing patterns of receptor activation, and do not completely activate or inhibit the receptors like orthosteric agonists or antagonists and have the ability to fine tune the receptor activity. A second potential advantage of receptor

modulation by allosteric agents, is that they only alter the sensitivity of the receptors and allow the system to react in a more normal physiological way to the changing concentrations of the endogenous agonist. When the allosteric sites are completely occupied by ligand, no further effect can be obtained which lowers the possibility of unwanted side effects from overdose. On the other hand, when the orthosteric site is completely occupied by ligand other than the endogenous ones, the receptor might go to a fully stimulated or fully inhibited state and it becomes unresponsive to the effect of endogenous neurotransmitters.

The neurotoxic and pro-survival effects of NMDARs gives a very narrow therapeutic potential for prospective NMDAR targeting agents, and the remodeling of NMDARs according to the physiological conditions, further add to the difficulties. The most significant idea to hold in mind during development is to maintain the potentiating and inhibitory balance of NMDARs.

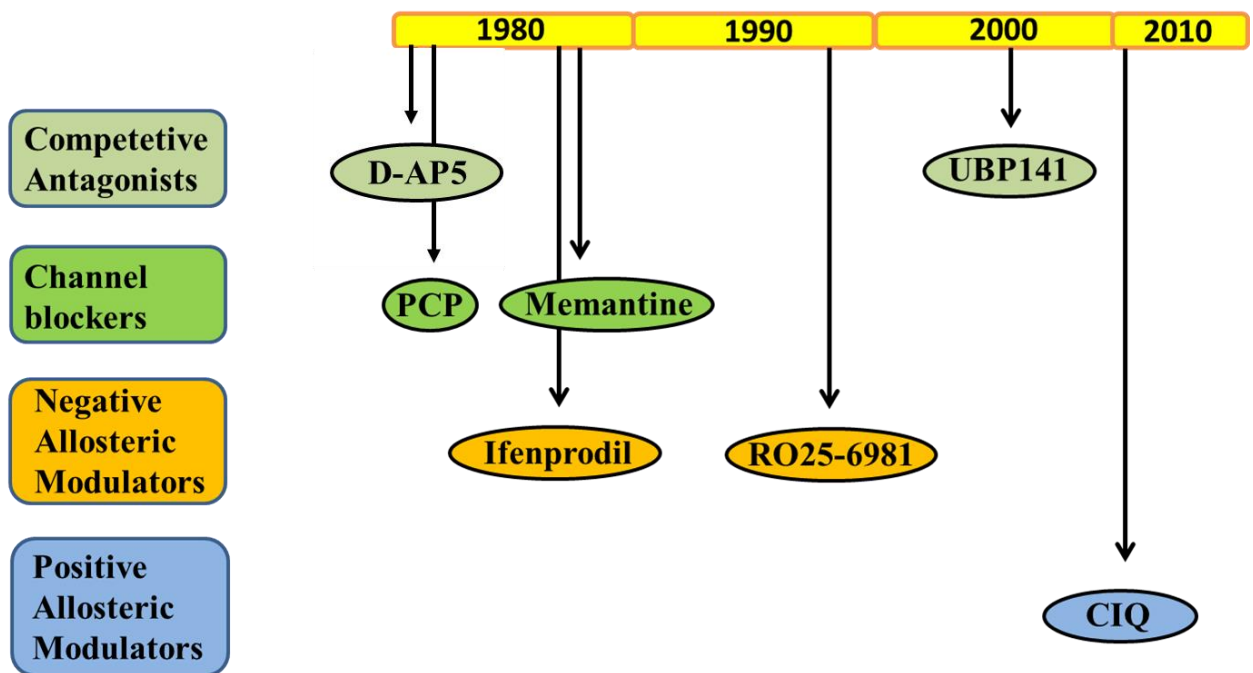


Figure 6 Strategies for NMDAR drug development over the past few years and potentially useful classes of drugs.

F. Pregnenolone sulfate

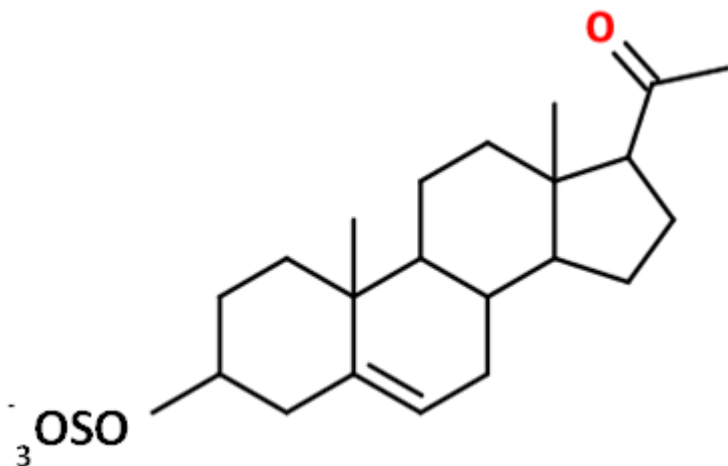


Figure 7: Chemical structure of pregnenolone sulfate

Pregnenolone sulfate (PS) is an endogenous neurosteroid which can be synthesized de novo from precursor cholesterol (Baulieu et al., 2001). The extracellular loop between TM3, TM4 and M4 domain has been identified as the binding site for pregnenolone sulfate, also known as Steroid Modulatory Domain 1 (SMD1) (Jang et al., 2004; Horak et al., 2006; Schumacher et al., 2007). In studies which were carried out using NMDARs expressed in *Xenopus* oocytes, it was found that PS showed potentiation of NMDAR current at GluN1/GluN2A and GluN1/GluN2B receptors and inhibition of NMDAR current at GluN1/GluN2C and GluN1/GluN2D receptors (Malayev et al., 2002). Thus, the effect of PS on NMDARs is found to be subtype-dependent. PS is also found to slow the deactivation kinetics in HEK cells for GluN1/GluN2A and GluN1/GluN2B receptors (Ceccocon et al., 2001) Further complicating the story, it is also shown that pre-application

of PS, showed a much larger potentiation as compared to co-application at GluN1/GluN2B receptors (Horak et al., 2004). However, PS is found to inhibit AMPA and kainite receptors (Wu et al., 1991). PS activity is found to be affected by the splice variants of GluN1 subunit. GluN1b subunit differs from the GluN1a subunit, by the presence of an exon-5 at the ATD. It was found that PS induced potentiation of NMDAR currents, specifically at GluN1/GluN2A receptors was observed in the presence of exon-5. Moreover, this effect was also pH dependent, with potentiation observed with a decrease in pH at GluN1/GluN2A receptors. Kostakis et al concluded that PS relieves the tonic proton inhibition observed with reduced pH in the presence of exon-5 (Kostakis et al., 2011). It is also assumed that the potentiating and inhibitory effects could be mediated by different binding sites altogether (Park-Chung et al., 1997; Horak et al., 2006). Pregnenolone sulfate also shows a typical tail current with a slight increase in response before the application of agonists end, as seen in fast-jumps. This tail current is representative of NMDA ion-channel blocking agents. It basically implies that, if there are two distinct binding sites for PS, it might be dissociating from the inhibiting site, sooner than the dissociation from the potentiating site (Horak et al., 2006). The tail current might also represent slower dissociation of glutamate and glycine, as PS slows the deactivation kinetics (unbinding of agonists from the receptors).

G. Kinetic modeling for NMDARs

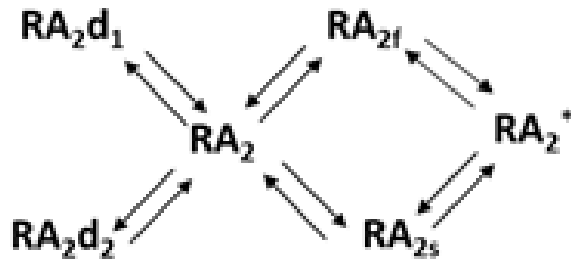


Figure 8: Physical model of NMDA receptor activation as proposed by Banke and Traynelis.

It is shown that prior to channel opening for NMDARs, they undergo multiple conformational changes (Banke and Traynelis., 2003). The open probability of GluN2A is higher than GluN2B. This could be due to the conformational changes proceeding more quickly for GluN2A than for GluN2B receptors, leading to faster opening of the GluN1/GluN2A receptors (Erreger et al., 2005). As shown by Banke and Traynelis, a fast (represented as f) and a slow transition (represented as s) state occurs before the receptor actually opens. The faster transition is controlled by the GluN1 subunit and the slower component is found to be controlled by the GluN2 subunit. They have also proposed that the fastest shut time component which corresponds to about 0.1ms, reflects the movement of the receptor channel from open to a closed state, however without reversal of any conformational change. The brief shut time component which is around 0.7ms reflects the movement of receptor from the open state to the closed state, with reversal of GluN1 subunit conformational change and the slower shut time component which corresponds to about 13ms reflects the conformational change controlled by the GluN2 subunit.

Schorge et al., 2005, predict the shut time can be resolved into two short-lived and one long-lived component representing the closed state of the receptor. They believe that

the short-lived components occur due to flipping of either GluN1 or GluN2 subunit. The long-lived components occur due to flipping of both GluN1 and GluN2 subunits. Here flipping refers to the conformational change that occurs prior to the opening of the receptor as also suggested by Burzomato et al., 2004. However, the two short-lived components are independent of each other and do not seem to affect each other.

The selection of a model for kinetic analysis is generally based on the log-likelihood generated by the model. Zhou and Auerbach analyzed a series of around 15 models, comprising at least three non-conducting and two conducting states. Based on the log-likelihood values, they came up with the following conclusions:

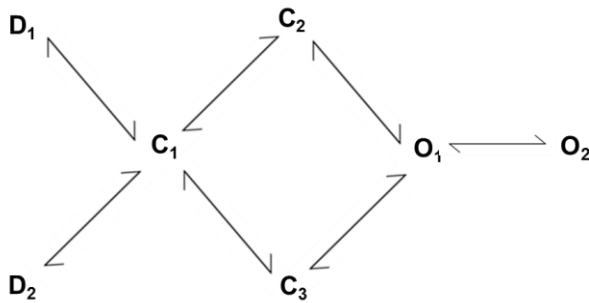


Figure 9: Cyclic model for NMDAR activation as proposed by Zhou and Auerbach.

- A kinetic model must contain at least three non-conducting (closed states) and at least two conducting states (open states).
- The conducting and non-conducting states should not have more than one path to move from one state to the other.
- The conducting states should be coupled to each other.
- The model should have at least two pre-opening, non-conducting states (desensitized states).

Chapter 2

**Bidirectional effect of pregnenolone sulfate on
GluN1/GluN2A NMDA receptor gating depending
on extracellular calcium and intracellular milieu**

A. ABSTRACT:

Pregnenolone sulfate (PS) is one of the most commonly occurring neurosteroids in the central nervous system and influences function of several receptors. PS modulates NMDA receptors (NMDARs) and has been shown to have both positive and negative modulatory effects on NMDAR currents generally in a subtype-selective manner. We assessed the gating mechanism of PS modulation of GluN1/GluN2A receptors transiently expressed in HEK 293 cells using whole-cell and single-channel electrophysiology. Only a modest effect on the whole-cell responses was observed by PS in dialyzed (non-perforated) whole-cell recordings. Interestingly, in perforated conditions, PS was found to increase the whole-cell currents in the absence of nominal extracellular Ca^{2+} whereas PS produced an inhibition of the current responses in the presence of 0.5 mM extracellular Ca^{2+} . The Ca^{2+} -binding DRPEER motif and GluN1 exon-5 were found to be critical for the Ca^{2+} -dependent bidirectional effect of PS. Single-channel cell-attached analysis demonstrated that PS primarily affected the mean open time to produce its effects, with positive modulation mediated by an increase in duration of open time constants while negative modulation mediated by a reduction in the time spent in a long-lived open state of the receptor. Further kinetic modeling of the single-channel data suggested that the positive and negative modulatory effects are mediated by different gating steps which may represent GluN2 and GluN1 subunit-selective conformational changes respectively. Our studies provide a unique mechanism of modulation of NMDARs by an endogenous neurosteroid which has implications for identifying state-dependent molecules.

B. INTRODUCTION:

Excitatory neurotransmission mediated by N-methyl-D-aspartate receptors (NMDARs) is known to play an important role in synaptic plasticity, learning and memory (Traynelis et al., 2010). Moreover, NMDAR dysfunction may contribute to a variety of neuropsychiatric and neurological disorders including schizophrenia, epilepsy, stroke and trauma (Hedegaard et al., 2012). NMDARs are tetramers composed of two obligatory glycine binding GluN1 subunits and usually two glutamate binding GluN2 subunits. There are four types of GluN2 subunits, GluN2A-GluN2D. The function of NMDARs is regulated by endogenous modulators such as magnesium, protons, zinc and neurosteroids (Traynelis et al., 2010). Pregnenolone sulfate (PS) is one of the most abundant neurosteroids formed by cleavage of cholesterol side chain in glial cells (Robel and Baulieu, 1994) and potentiates or inhibits the NMDARs in a subtype-selective manner (Malayev et al., 2002; Horak et al., 2006).

Initial studies in spinal cord neurons suggested that PS potentiation was dependent on the agonist concentration, with the potentiation being reduced at higher agonist concentrations and almost eliminated at 1 mM NMDA (Wu et al., 1991). Based on the agonist-concentration dependent effect it has been suggested that PS increases the agonist efficacy/potency (Malayev et al., 2002). In oocyte experiments where PS is co-applied with agonists, PS typically potentiates GluN1/GluN2A currents (Yaghoubi et al., 1998; Malayev et al., 2002). However, in fast jump experiments in mammalian expression system (HEK 293 cells) co-application of PS with agonists has been found to typically slow the desensitization and deactivation kinetics of GluN1/GluN2A receptors but not to increase the steady state currents (Ceccon et al., 2001; Horak et al., 2006). In contrast, pre-application of PS followed by agonist application leads to significant increase in the peak

amplitude of GluN1/GluN2A currents (Bowlby, 1993; Horak et al., 2004). These studies indicate that the effect of PS is partly disease-dependent. Overall, the effect of PS on GluN1/GluN2A receptors when co-applied with agonists differ in mammalian expression system compared to oocyte expression system and this discrepancy has not yet been resolved although it may involve the phosphorylation state of the receptor (Petrovic et al., 2009). Studies using site-directed mutagenesis and chimeric receptors suggest that the linker regions connecting the transmembrane (TM) 3 and 4 to the S2 domain of the ligand-binding domain and part of the TM3 and TM4 is a critical site of action of neurosteroids including PS (Horak et al., 2006; Jang et al., 2004). The action of PS has also been found to be mediated partly by relief of proton inhibition at GluN2A- and GluN2D-containing receptors but not GluN2B- and GluN2C-containing receptors (Kostakis et al., 2011).

The effects of PS on single-channel kinetics and gating of NMDARs remain poorly understood. Using whole-cell and cell-attached electrophysiology we have identified a novel aspect of PS action. Specifically, our studies indicate an extracellular Ca^{2+} - and intracellular milieu-dependent actions of PS which may provide novel insights into the positive and negative modulatory effects of PS. These novel paradigms also have important implications for our understanding of the physiological roles of PS.

C. MATERIALS AND METHODS:

Expression of recombinant NMDARs: Human embryonic kidney (HEK) 293 cells were maintained as previously described (Dravid et al., 2008). The cells were transiently transfected with ViafectTM reagent (Promega Corporation, Madison, WI). Rat GluN1-1a

(Genbank U11418, U08261; pCIneo vector; hereafter GluN1, provided by Dr. Stephen Heinemann), GluN2A (Genbank D13211, pCIneo vector, provided by Dr. Shigetada Nakanishi), and green fluorescent protein (GFP) in the ratio of 1:2:0.5 were used as previously described (Bhatt et al., 2013). The GluN1-1b splice variant and GluN1-1a-R663A mutant were provided by Dr. Stephen Tryanellis and GluN2B (Genbank U11419, Q00960; pcDNA3.1 vector) was provided by Dr. Peter Seeburg (Max Planck Institute for Medical Research, Heidelberg, Germany). Electrophysiology experiments were performed 16–48 hours after transfection.

Electrophysiology: Electrophysiological recordings in whole-cell and single-channel mode were obtained from transfected HEK 293 cells at room temperature (22–25°C). An external solution containing (in mM) 150 NaCl, 3 KCl, 10 HEPES, 0.5 CaCl₂ and 6 mannitol (to adjust osmolarity) was used for the recordings unless otherwise stated. Recordings were conducted in the absence of nominal extracellular CaCl₂ or in the presence of 0.5 mM CaCl₂ as indicated in the text for each experiment. The external pH was adjusted to 7.4 with NaOH. This solution was supplemented with 0.02 mM EDTA to chelate trace amounts of zinc. The same external solution was used for whole-cell recordings, as well as cell-attached recordings. Recordings were performed under two conditions: (1) 100 μM glutamate, 100 μM glycine (control patches); and (2) 100 μM glutamate, 100 μM glycine and 100 μM PS (PS patches). Pregnenolone sulfate (3β-Hydroxy-5-pregnen-20-one 3-sulfate or 3-Hydroxypregn-5-en-20-one sulfate or 5-Pregnen-3β-ol-20-one sulfate) sodium salt was obtained from Sigma-Aldrich. For whole-cell recordings, agonists and PS were added to the extracellular solution, and for cell-attached recordings, these drugs were present only in the pipette solution. Recordings were

obtained using an Axopatch 200B amplifier (Axon Instruments/Molecular Devices) and digitized with pCLAMP 10 software (Axon Instruments/Molecular Devices). Whole-cell recordings were obtained at -70 mV, filtered at 2 kHz, and digitized at 5 kHz. For cell-attached recordings a potential (V_m) of +70 mV was applied and data were filtered at 5 kHz (-3 dB, 8-pole Bessel) and digitized at 20 kHz. Single-channel amplitude was not corrected for junction potential.

The internal solution used for whole-cell recordings consisted of (in mM) 110 cesium gluconate, 30 CsCl₂, 5 HEPES, 4 NaCl, 0.5 CaCl₂, 2 MgCl₂, 5 BAPTA, 2 Na₂ATP, and 0.3 Na₂GTP (pH 7.3). For perforated whole-cell patch-clamp recordings 20 µg/ml of gramicidin was added to the pipette internal solution. Whole-cell configuration after gigaohm seal was reached typically within 10-15 minutes. Rapid perfusion for whole-cell concentration jumps was achieved with a two-barreled theta glass pipette controlled by a piezoelectric translator (Burleigh). The solution exchange times for 10–90% solution were typically ~1-2 ms. Two concentration profiles were obtained: (1) 100 µM glutamate, 100 µM glycine, and (2) 100 µM glutamate, 100 µM glycine and 100 µM PS. The cell was moved from the control solution with no drugs to a solution containing agonists ± PS. Drug application was typically for 2.5 s during each 15 s sweep.

D. DATA PROCESSING AND KINETIC MODELING:

Recordings containing a single active channel were idealized using QUB software (www.qub.buffalo.edu) as previously described (Bhatt et al., 2013; Dravid et al., 2008). The idealized data was used for maximum interval likelihood fitting (MIL; Qin et al., 1996). A 120 µs dead time was imposed using QUB. All gating steps were free and not

constrained. The C5O2 model consisting of 3 closed and 2 open states in linear configuration and two desensitized states emerging from C1 and C2 respectively (Figure 7) provided the best fit to the single channel data based on the log likelihood values. Other models tested included a C4O2 model with four instead of five closed states and a model where the receptor can transition to either a fast or slow gating step as described previously (Bhatt et al., 2013). The mean open time, mean shut time and open probability was obtained from the idealized data using ChanneLab (www.synaptosoft.com), with an imposed dead time of 120 μ s. Peak and steady state responses and deactivation, and desensitization time course for whole-cell recordings were analyzed using Clampfit (pClamp 10.2).

Statistical Analysis: All the values are expressed as mean \pm SEM. Data were compared using paired *t*-test for macroscopic current profiles and unpaired *t*-test for the cell-attached patches. Values of $P\leq 0.05$ were considered significantly different.

E. RESULTS:

Effect of pregnenolone sulfate on macroscopic currents is dependent on intracellular milieu and extracellular calcium

We tested the effect of PS on macroscopic GluN1/GluN2A whole-cell currents under dialyzed (non-perforated) conditions. PS (100 μ M) was co-applied with glutamate (100 μ M) and glycine (100 μ M) (Figure 1) to determine the optimum conditions for carrying out single-channel studies. PS (in the absence of nominal extracellular Ca^{2+}) was found to produce a modest but significant reduction in the peak response ($p=0.0285$, $N=6$, paired *t*-test, $I_{\text{PS}}/I_{\text{control}} = 0.898\pm 0.021$) with no significant effect on the steady state responses ($p=0.1037$, $I_{\text{PS}}/I_{\text{control}} = 0.855\pm 0.040$). We further tested whether extracellular

Ca^{2+} is a factor for absence of strong responses to PS. In the presence of 0.5 mM Ca^{2+} , PS was found to have no significant effect on the peak response ($p=0.1481$, $N=5$, $I_{\text{PS}}/I_{\text{control}}=1.050\pm 0.082$) or steady state responses ($p=0.0669$, $I_{\text{PS}}/I_{\text{control}}=1.086\pm 0.063$).

Previous studies which have evaluated the effect of co-applied PS on whole-cell GluN1/GluN2A currents in HEK 293 cells have found modest or no potentiation of steady state currents when co-applied with agonists (Ceccon et al., 2001; Horak et al., 2006). Thus our findings in whole-cell conditions are similar to these studies. In oocyte recordings, however, an increase in GluN1/GluN2A responses is consistently observed where unlike whole-cell recordings the intracellular milieu is generally undisturbed. It has previously been shown that NMDAR responses and their modulation by endogenous or synthetic molecules is affected by phosphorylation and dephosphorylation pathways (Acker et al., 2011; Petrovic et al., 2009). In a typical whole-cell recording dialyzing the intracellular components might affect the phosphorylation/dephosphorylation machinery of the cell. Hence we performed perforated whole-cell recordings using gramicidin to test whether keeping intracellular milieu intact would affect PS modulatory actions. Under perforated whole-cell conditions and in the absence of extracellular Ca^{2+} , PS significantly increased the peak response ($p=0.00104$, $N=7$, $I_{\text{PS}}/I_{\text{control}}=1.814\pm 0.073$) and the steady state response ($p=0.0019$, $I_{\text{PS}}/I_{\text{control}}=1.818\pm 0.097$). In the presence of 0.5 mM extracellular Ca^{2+} , in perforated patch mode PS significantly reduced the peak response ($p=0.0083$, $N=7$, $I_{\text{PS}}/I_{\text{control}}=0.60\pm 0.036$) and the steady state response ($p=0.0124$, $I_{\text{PS}}/I_{\text{control}}=0.582\pm 0.025$). PS did not significantly affect the desensitization or deactivation time constants under any of the conditions tested (data not shown). A transient rise in current was observed in the whole-cell recordings when the solution containing PS was washed-out (Figure 1). This

feature is similar to that demonstrated previously when PS and agonists are co-applied (Horak et al., 2004).

Molecular determinants of Ca²⁺-dependent inhibition by pregnenolone sulfate

We further assessed the potential molecular determinants of extracellular Ca²⁺-dependent inhibition by PS. We first replicated the observation of inhibition of GluN1/GluN2A currents by PS in the presence of 0.5 mM external Ca²⁺ under perforated whole-cell recording conditions (Figure 2A). One of the sites where Ca²⁺ binds in the extracellular vestibule is the DRPEER motif (Watanabe et al., 2002; Karakas and Furukawa, 2014). We tested the effect of PS on GluN1R663A/GluN2A receptors in perforated whole-cell patch clamp recordings. This mutant was chosen based on its most exterior positioning, which may prevent it from having basal effects (as indicated in Watanabe et al., 2002) yet may allow for testing the importance of this region in the modulatory effect of PS. We found that PS potentiated the peak current ($p=0.0389$, $N=5$, $I_{PS}/I_{control}=1.654\pm 0.191$) as well as the steady-state current responses ($p=0.0264$, $N=5$, $I_{PS}/I_{control}=1.543\pm 0.138$) from GluN1R663A/GluN2A receptors in the presence of 0.5 mM Ca²⁺ (Figure 2B). The degree of potentiation was comparable to the potentiation by PS in the absence of nominal Ca²⁺. This finding demonstrates a critical role of the DRPEER motif in the bidirectional effect of PS depending on extracellular Ca²⁺. We further tested the effect of exon-5 insert (present in GluN1-1b) which is a key molecular determinant for proton and zinc inhibition (Traynelis et al., 2010) as well as proton-dependent differential efficacy of PS at GluN1/GluN2A versus GluN1/GluN2B receptors (Kostakis et al., 2011). The whole-cell responses at GluN1-1b/GluN2A receptors were

significantly increased by PS in the presence of 0.5 mM Ca^{2+} (Figure 2C). showing an increase in the peak current ($p=0.0357$ $N=7$, $I_{\text{PS}}/I_{\text{control}}=1.525\pm0.105$; as well as steady state current responses ($p=0.0199$ $N=7$, $I_{\text{PS}}/I_{\text{control}}=1.360\pm0.11$) PS was also found to increase the deactivation kinetics of the GluN1-1b/GluN2A receptors (data not shown). Together these data demonstrate that conformational changes induced by presence of exon-5 can mask the inhibitory effect of PS produced due to its allosteric interaction with Ca^{2+} binding at the DRPEER motif. It should however be noted that we cannot rule out other possibilities such as a change in proton-sensitivity of the receptor leading to changes in the mechanism of action of PS. Finally we tested whether the Ca^{2+} -dependent inhibition is specific for GluN2A-containing receptors. In contrast to GluN1/GluN2A receptors, no significant inhibition by PS was observed in the presence of Ca^{2+} at the GluN1/GluN2B receptors ($N=5$; Figure 2D), although no potentiation was observed either. However, PS did significantly increase the decay kinetics of the GluN1/GluN2B receptors (data not shown).

Pregnenolone sulfate affects mean open time of GluN1/GluN2A receptors

After identifying the conditions where the potentiating and inhibiting effects of PS are robust we assessed the single-channel effects of PS under these conditions. We obtained cell-attached patches with one-active channel for evaluating the effect of PS on GluN1/GluN2A gating (Figure 3). In the first set of recordings CaCl_2 was absent from the pipette internal solution. The mean open time ($\pm\text{SEM}$) in control patches was found to be 1.52 ± 0.17 ms (114,675 events; $N=9$). In the presence of PS the mean open time was significantly higher 3.11 ± 0.24 ms (93,505 events; $N=5$, $p=0.00017$, unpaired t -test). The mean shut time was not affected by PS; 17.3 ± 1.8 ms in control patches (115,032 events)

and 15.3 ± 2.9 ms in PS patches (93,840 events, $p=0.528$). The open probability, measured over the entire length of recordings, was found to increase from 0.082 ± 0.007 in control patches to 0.186 ± 0.034 in PS patches ($p=0.0022$). The amplitude of openings was unaffected by PS, with amplitude being 5.01 ± 0.18 pA for control patches and 5.09 ± 0.16 pA for PS. Thus it appears that the major effect of PS is on the mean open time of the GluN1/GluN2A receptors which leads to higher open probability in the presence of PS. Compared to previous studies the overall open probability of GluN1/GluN2A was found to be lower in our cell-attached patches. This may be due to differences in the recording solutions, mode of recording or difference in the modal gating of the receptor. However, it should be noted that under our recording conditions the mean open time and open probability for GluN1/GluN2A is higher compared to GluN1/GluN2B (Bhatt et al., 2013), with a similar order of magnitude as previously described in outside-out patches (Erreger et al., 2005).

Upon inclusion of 0.5 mM Ca^{2+} in extracellular solution, PS was found to reduce the mean open time from 1.53 ± 0.18 ms (57,406 events; $N=5$; Figure 4) in control patches to 0.72 ± 0.07 ms (85,892 events; $N=6$, $p=0.0012$, unpaired t -test). No significant change in mean shut time was observed in control patches; 19.3 ± 2.0 ms (57,824 events) versus PS patches; 19.4 ± 3.9 ms (85,903 events) ($p=0.981$). The overall open probability was found to be significantly reduced by PS in the presence of 0.5 mM Ca^{2+} . The open probability in control patches was 0.076 ± 0.012 which was significantly reduced in the presence of PS to 0.041 ± 0.006 ($p=0.023$). The amplitude of openings was unaffected by PS in the presence of extracellular Ca^{2+} (control= 5.24 ± 0.28 pA; PS= 5.27 ± 0.28 pA). Since no change in mean shut time was seen, the reduction in open probability was primarily due to shorter mean

open time. No significant differences in single-channel properties were observed in control patches obtained under conditions of absence or presence of extracellular 0.5 mM Ca^{2+} . Thus extracellular Ca^{2+} bi-directionally modulates PS responses similar to results obtained in perforated whole-cell recordings.

Pregnenolone sulfate produces unique effects on open and shut time constants which underlie potentiation and inhibition of GluN1/GluN2A receptors

We further evaluated the effect of PS on the open and shut time characteristics. We fitted the single-channel data from individual patches using MIL to a model consisting of two open states and five shut states of which two were the longer desensitized states as previously described (Dravid et al., 2008). Both control and PS patches produced reasonably good fits with this scheme suggesting this model provides a reasonable description of the receptor gating (assuming that in the presence of 100 μM PS the receptor binding sites for PS are close to 100% occupied). We first compared the patches obtained in the absence of extracellular Ca^{2+} which showed ~ 2 -fold potentiation in the open probability. The global fit for all events in the absence of extracellular Ca^{2+} is presented in Figure 5 and the time constants and area of individual patches are presented in Table 1. A major effect of PS as evident from this analysis is an increase in time constants for the open states (control, $\tau_1=0.31\pm 0.04$, $\tau_2=1.76\pm 0.26$; PS, $\tau_1=0.86\pm 0.27$ ($p=0.0179$), $\tau_2=3.62\pm 0.37$ ($p=0.0013$)). The shift in time constants is consistent with an increase in the mean open time observed in the presence of PS (Figure 3). No significant change was observed in the areas of open states. Analysis of shut time constants revealed that the time constants τ_2 , τ_3 and τ_5 were significantly different (Table 1). The τ_2 ($p=0.0014$) and τ_3 ($p=0.0038$) were

reduced in the presence of PS while τ_5 ($p=0.0044$) was significantly increased. No change in the area of shut time constants was observed except that of τ_5 which was reduced in the presence of PS ($p=0.0351$).

We next evaluated the effect of PS on open and shut times in the presence of 0.5 mM extracellular Ca^{2+} (Figure 6; Table 1). As clearly evident a significant reduction in the areas of the longer time constant τ_2 ($p=0.00002$) and an increase in areas of τ_1 ($p=0.00002$) was found in the presence of PS, however, no change of the time constants themselves was observed (control, $\tau_1=0.39\pm 0.09$ ($22\pm 7\%$), $\tau_2=1.70\pm 0.21$ ($78\pm 7\%$); PS, $\tau_1=0.50\pm 0.04$ ($87\pm 5\%$), $\tau_2=2.30\pm 0.61$ ($13\pm 5\%$)). These results suggest that the primary inhibitory effect of PS is via reduction in the dwell time in the longer open state. No significant differences were observed in the shut time constants except τ_1 which was significantly increased in the presence of PS ($p=0.0417$) (Table 1). Previous studies suggest that the shut time components consisting of τ_2 and τ_3 likely represent a conformational change in the GluN2 subunit and that in τ_1 may represent a conformational change in the GluN1 subunit (Banke and Traynelis, 2003; Erreger et al., 2005). Thus the specific changes in τ_2 and τ_3 by PS in the absence of extracellular Ca^{2+} may indicate GluN2-selective conformational change while specific change in τ_1 in the presence of 0.5 mM Ca^{2+} may represent conformational change in GluN1 subunit.

Pregnenolone sulfate influences different gating steps to produce potentiation and inhibition of GluN1/GluN2A receptors

We addressed the specific effect of PS on the gating steps during receptor activation using a model previously described for NMDARs including GluN1/GluN2A receptors

(Dravid et al., 2008; Kussius and Popescu, 2009). MIL fitting to the model demonstrated that in the absence of nominal Ca^{2+} , PS increased the rates for forward steps $\text{C}_1 \rightarrow \text{C}_2$ ($p=0.0025$) and $\text{C}_2 \rightarrow \text{C}_3$ ($p=0.0264$) and the reverse step $\text{C}_2 \rightarrow \text{C}_1$ ($p=0.0075$) (Table 2). The reverse rate constant from $\text{O}_1 \rightarrow \text{C}_3$ was reduced in the presence of PS ($p=0.0004$). These findings are also predicted by the changes in open time constants τ_1 and τ_2 and shut time constants τ_2 and τ_3 (Table 1). In contrast, PS in the presence of 0.5 mM Ca^{2+} , which reduces open probability and mean open time, lead to an increase in the rate of reverse gating step from $\text{O}_1 \rightarrow \text{C}_3$ ($p=0.0117$) and a dramatic reduction in the forward $\text{O}_1 \rightarrow \text{O}_2$ ($p=0.0029$) rate constant which is predicted by a reduction in the area of the open time constant τ_2 (Table 1). These results indicate that the positive and negative modulatory effects of PS may not be mediated via effects on the same gating steps.

F. DISCUSSION:

In this study we found that in dialyzed whole-cell recordings, PS produced only modest effects on the steady state currents from GluN1/GluN2A receptors, however, the effect of PS was significantly different in perforated whole-cell recordings where the intracellular milieu is likely to be closer to the native system. Under perforated conditions, PS was found to cause potentiation of steady state currents in the absence of Ca^{2+} and inhibition in the presence of 0.5 mM Ca^{2+} . In single-channel cell-attached recordings, PS was similarly found to produce bi-directional effects depending on extracellular Ca^{2+} . When PS was co-applied with agonists in the absence of Ca^{2+} , PS led to an increase in the open probability whereas in the presence of 0.5 mM Ca^{2+} , PS led to a reduction in the open probability of GluN1/GluN2A receptors.

Mechanism for positive and negative modulatory effects of pregnenolone sulfate

It has been shown that the action of PS on NMDARs is phosphorylation-dependent and therefore intracellular milieu may affect PS-mediated modulation. Previous studies have reported PS modulation to be mediated partly by protein kinase A (PKA) (Petrovic et al., 2009). The potentiating effect of PS in outside-out patches is lost after 2 minutes of obtaining the patch and this effect can be reversed by addition of PKA (Petrovic et al., 2009). Thus one possibility is that the potentiating effect on steady state currents is lost in dialyzed whole-cell mode due to inhibition of intracellular PKA or other changes that affect NMDAR post-translational modifications. This phenomenon of intracellular milieu-dependent effects may also be true for other agents. Recent studies have demonstrated that the IC_{50} of a subtype-selective negative allosteric modulator DQP-1105 is dependent on whole-cell configuration. It was found that the inhibitory action of DQP-1105 was reduced at GluN1/GluN2A receptors and a greater magnitude of subtype-selectivity between GluN1/GluN2D and GluN1/GluN2A receptors was observed in perforated mode of recording using gramicidin compared to under dialyzed condition (Acker et al., 2011). Also of note, the whole-cell dialyzed configuration is known to increase the desensitization of the NMDAR (Sather et al., 1990). Since GluN2A-containing receptors have greater desensitization while GluN2D-containing receptors appear to lack desensitization (Traynelis et al., 2010) it is likely that the difference in open probability in the two-preparations for the two subtypes may also underlie the differential effect of DQP-1105. This may also be relevant to the differential effect of PS in dialyzed and perforated conditions in the present study.

Our data suggest that 0.5 mM Ca^{2+} is sufficient to switch PS modulation from positive to negative effect under perforated whole-cell mode and in cell-attached recordings (Figure 1, 2, 3, 4). Thus the potential site of Ca^{2+} binding or action may provide understanding of the inhibitory site of PS. Two Ca^{2+} binding sites have been identified in the NMDARs. One is present in the pore of a functional NMDAR (Jahr and Stevens, 1993). The other Ca^{2+} binding site is present in the DRPEER region located in the linker region between the ligand binding domain (LBD) and transmembrane domain (TMD) of the GluN1 subunit (Watanabe et al., 2002). Both sites have been shown to increase the Ca^{2+} -block of the channel and reduce the channel conductance (Jahr and Stevens, 1993; Watanabe et al., 2002). However, we did not find a significant change in single-channel amplitude under control 0.5 mM Ca^{2+} conditions or with PS, which only reduced the mean open time. Thus the inhibitory mechanism of external Ca^{2+} alone appear to be different from the inhibitory effect of PS. Using GluN2A and GluN2C chimeras and site-directed mutagenesis it has been shown that PS does not act by binding to the amino terminal domain (ATD), LBD and intracellular carboxyl-terminal domain (CTD) of GluN2A receptors (Cameron et al., 2012; Horak et al., 2006). It exerts its effect by acting on TM3-TM4 loop of the NMDARs (Borovska et al., 2012; Horak et al., 2006; Park-Chung et al., 1997). Additionally, in oocyte studies the potentiating effect of PS on GluN1/GluN2A receptors is influenced by the presence or absence of exon-5 in the GluN1 subunit. In the absence of exon-5 (GluN1-1a, which we have used) the potentiation by PS is lower compared to when exon-5 is present (GluN1-1b) (Kostakis et al., 2011). This finding is relevant to the location of DRPEER Ca^{2+} -binding site on the GluN1 subunit. Thus the Ca^{2+} -dependent effects of PS may arise due to an allosteric interaction between Ca^{2+} -binding to

the DRPEER site and PS binding to an “inhibitory site” influenced by GluN1 subunit which together reduce the stability of long-lived open times. In contrast, the absence of Ca^{2+} prevents this allosteric interaction and inhibitory action of PS. Our results with the GluN1R663A mutant in the DRPEER motif and exon-5 insert are in agreement with this hypothesis since PS instead of inhibiting responses in the presence of 0.5 mM Ca^{2+} led to potentiation of the receptor to a similar extent as in the absence of nominal Ca^{2+} .

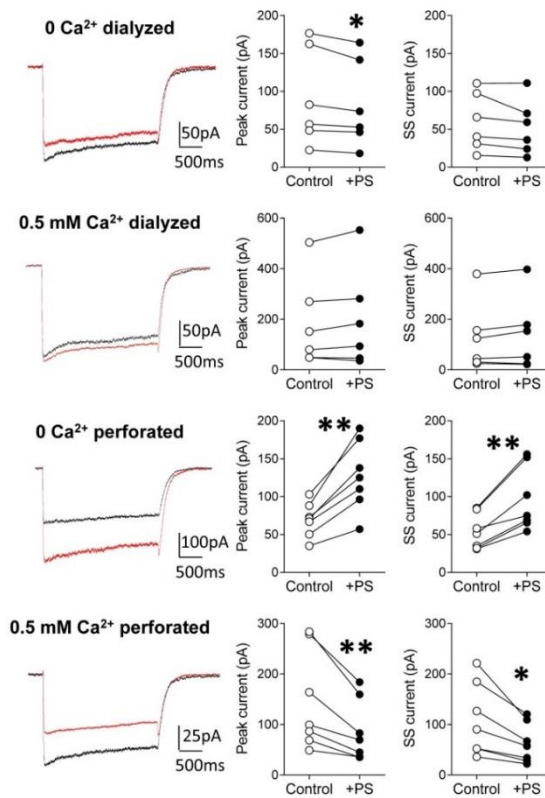
Bidirectional actions of pregnenolone sulfate are produced by mechanistically distinct gating steps

Our single-channel data demonstrates a significant effect of PS on mean open time in producing both inhibition and potentiation of the receptor. This is most evident in the free-energy plots where effects on open time are most predominant (Figure 7). The properties of PS-induced inhibition are quite peculiar in that the longer open state is almost completely abolished. This correlates with a substantial reduction in the forward rate constant from O1 to O2 state in the kinetic scheme (from 920 to 70). Based on our kinetic analysis the pore dilation may occur in two distinct stable states as represented by O1 and O2. These states can occur in a sequential manner as we and others have represented in our kinetic models (Dravid et al., 2008; Kussius and Popescu, 2009) or these may emerge from two different closed states (Schorge et al., 2005). Based on our data PS interaction with Ca^{2+} obstructs the dilation of pore to a more stable conformation representing the longer open time. Removal of nominal Ca^{2+} or presumably preventing Ca^{2+} interaction with DRPEER site or masking the effect of Ca^{2+} with the exon-5 insert (Figure 1, 2) unravels the potentiating mechanism of PS. The potentiating mechanism engages molecular

determinants close to the TM3 and TM4 regions linker forming the external vestibule as demonstrated previously (Kostakis et al., 2011). Indeed restricting linkers in TM3-TM4 or use of reducing agent DTT which acts on GluN1 cysteines close to the TM3-TM4 linker (Sullivan et al., 1994) affects multiple gating steps not restricted to transitions to open states similar to our kinetic analysis of effect of PS in the absence of nominal Ca^{2+} (Talukder and Wollmuth, 2011). This difference in PS inhibition mainly affecting fast gating steps transitioning to open states while PS potentiation affecting slow gating steps in addition to transition to open states suggests that inhibitory site of action of PS may be closer to the pore or vestibule of the channel while the potentiating effect may involve structural elements involving larger and therefore slower conformational changes. Studies using GluN1 and GluN2 subunit partial agonists and Lurcher mutations suggest that a slower gating step may represent GluN2 subunit conformational change while a faster gating step may represent a GluN1 subunit conformational change (Banke and Traynelis, 2003; Erreger et al., 2005; Murthy et al., 2012). Thus based on our data it is possible that the potentiation of the receptor is mediated by modification of the slower putative GluN2-gating step since we observed changes in longer shut time constants τ_2 and τ_3 and slower gating steps in addition to its effect on mean open time. In contrast, the inhibition of the receptor by PS in the presence of 0.5 mM Ca^{2+} may involve modification to the GluN1-gating step since it led to a specific change in τ_1 . This hypothesis is also supported by our results in the DRPEER mutant and GluN1-1b splice variant where the PS inhibition is eliminated.

Conclusion and remaining questions

In most of the previous studies in neurons and mammalian expression system a potentiating effect is observed with pre-application of PS. In fact at GluN1/GluN2C receptors while co-application leads to PS-induced inhibition, pre-application of PS followed by agonist-alone application leads to potentiation of currents (Horak et al., 2006). Effect of pre-application is likely a more relevant phenomenon to normal CNS physiology since PS appears to be present under basal conditions (Robel and Baulieu, 1994). Thus future experiments to address the differences in whole-cell responses in dialyzed and perforated conditions upon pre-application of PS may reveal interesting results which may be relevant to neurosteroid physiology in the CNS. Interestingly, PS is also being evaluated for its efficacy for treating cognitive and behavioral impairments in mental disorders (for example Wong et al., 2015; Marx et al., 2014). Our data suggests that there is a need to better understand the pharmacological basis of actions of PS and to assess the ability of newly discovered allosteric modulators of NMDAR to serve as intracellular cell state-dependent agents.



G. FIGURES

Figure 1: Modulation of whole-cell responses by pregnenolone sulfate is dependent on intracellular milieu and extracellular calcium.

Whole-cell recordings under non-perforated (dialyzed) or perforated modes were obtained from HEK 293 expressing GluN1/GluN2A receptors in the absence of nominal Ca²⁺ or in the presence of 0.5 mM extracellular Ca²⁺ (holding potential = -70 mV, filtered at 2 kHz, digitized at 5 kHz). Agonists (100μM glutamate and 100μM glycine) were applied in the absence (black traces) or presence of 100μM PS (red traces) and the peak and steady state responses were evaluated. Responses were compared by paired *t*-test. *

denotes $P < 0.05$, $**P < 0.01$.

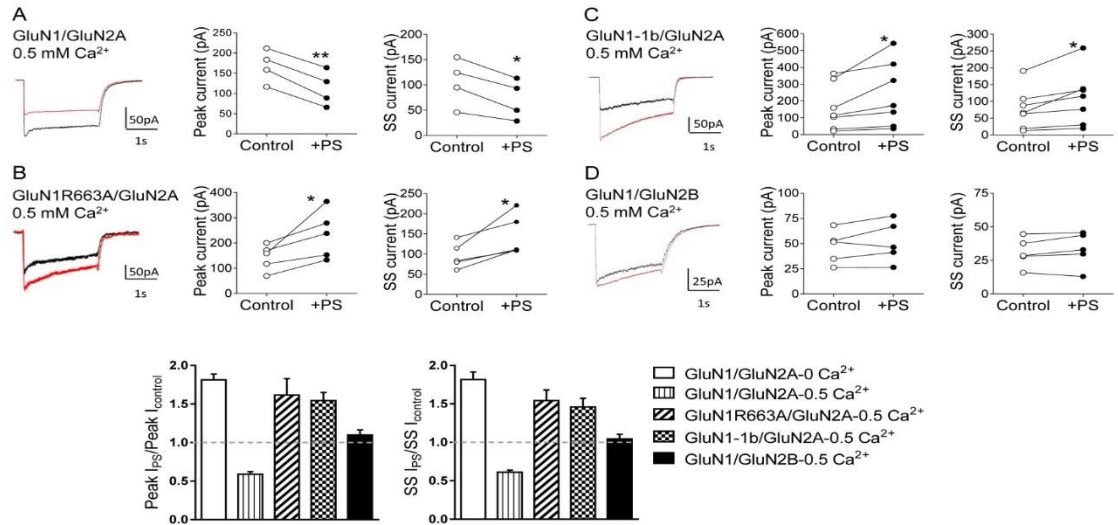


Figure 2: Molecular determinants of inhibition by pregnenolone sulfate in the presence of external Ca²⁺. **A.** PS (100 μ M) in the presence of extracellular 0.5 mM Ca²⁺ reduced the glutamate (100 μ M) + glycine (100 μ M) induced responses. PS potentiated current responses at **B.** GluN1R663A/GluN2A receptors as well as **C.** GluN1-1b/GluN2A receptors. **D.** PS did not inhibit current responses at GluN1/GluN2B but neither did it significantly increase the responses. Traces in black represent control with glutamate and glycine and traces in red represent responses in the presence of PS. Responses were compared by paired *t*-test. * denotes $P < 0.05$, $**P < 0.01$. **E.** Fold-change in current by PS relative to control is plotted as individual bars with 1 representing baseline.

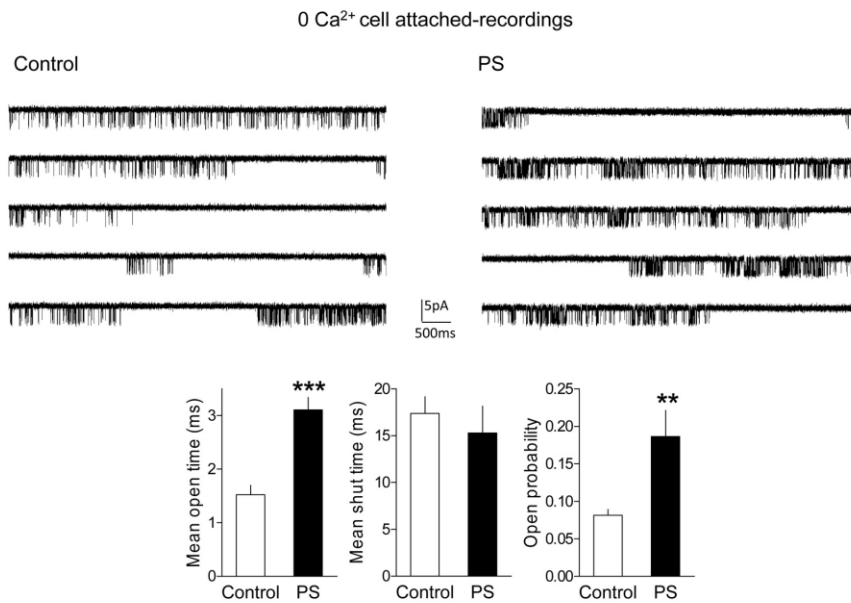


Figure 3: Pregnenolone sulfate increases open probability of GluN1/GluN2A receptors.

Representative steady state single-channel recording in cell-attached mode from patches containing one active GluN1/GluN2A receptor. Openings are downwards for all the traces. Recording was obtained at 100 μ M glutamate and 100 μ M glycine (Pipette potential = +70 mV, filtered at 5 kHz (2 kHz for presentation), digitized at 20 kHz) under control condition or in the presence of PS (100 μ M). PS (n=5) increased the mean open time of the receptor compared to control patches (n=9) (P=0.00017). PS did not have any significant effect on the mean shut time of the receptor (P=0.528). The probability of opening (calculated individually over the length of entire recording) was found to be significantly increased by PS (P=0.0022). Unpaired *t*-test was used for comparison. *** denotes P<0.001, **P<0.01.

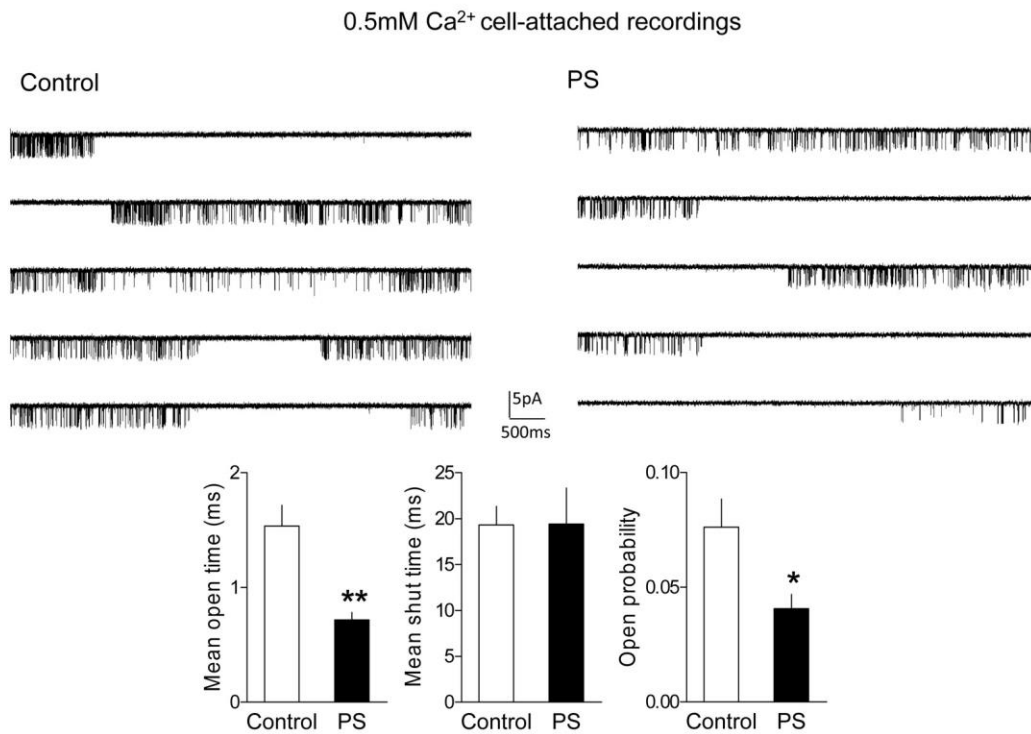


Figure 4: Effects of pregnenolone sulfate on the GluN1/GluN2A receptor single-channel properties is dependent on extracellular Ca²⁺.

Cell-attached recordings were obtained with addition of 0.5 mM Ca²⁺ to the pipette internal solution. Representative steady state single-channel control recordings from patches containing one active GluN1/GluN2A receptor with the absence or the presence of PS (100μM). PS (n=6) reduced the mean open time of the receptor compared to control patches (n=5) (P=0.0013). PS did not have any significant effect on the mean shut time of the receptor (P=0.981). The probability of opening was significantly reduced by PS (P=0.0229). Data are compared with unpaired *t*-test. ** denotes P<0.01, * denotes P<0.05.

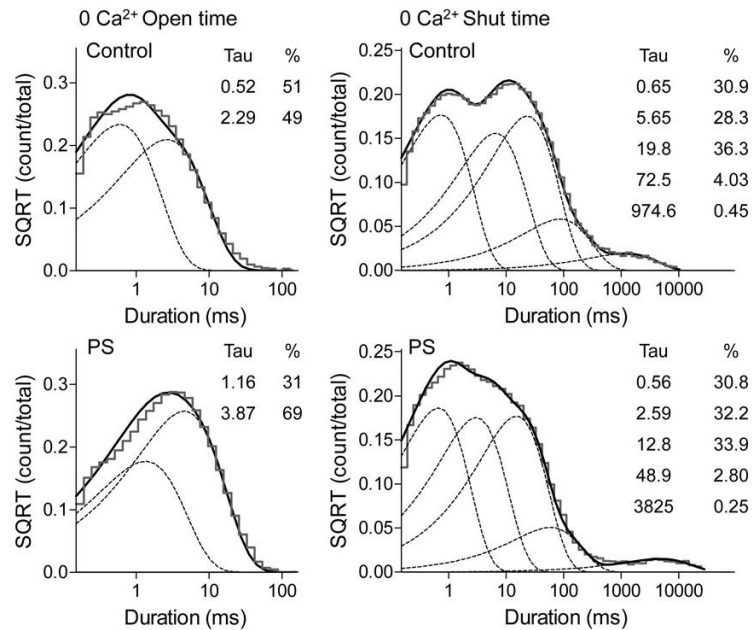


Figure 5: Pregnenolone sulfate mediated potentiation of GluN1/GluN2A receptors involves a shift in open states to longer durations and a reduction in the occupancy of long-lived shut states.

The single-channel currents from cell-attached patches in the absence of nominal Ca²⁺ with one active GluN1/GluN2A receptor were idealized for each patch and summed to generate global dwell time histograms. The open time histogram was fitted by a sum of two exponential components: control, 114,675 open events (n=9); PS, 93,505 events (n=5). The time constants and % area are shown in the inset. The dwell times from each patch were individually fitted and are presented in Table 1. PS was found to significantly increase τ_1 and τ_2 time constants but not the area (Table 1). The composite shut time histogram was fitted by a sum of five exponential functions: control, 115,032 closed periods (n=9); PS, 93,840 closed periods (n=5). PS was found to significantly reduce the τ_2 and τ_3 time constants and increase τ_5 (Table 1). Only the area of τ_5 was significantly reduced by PS.

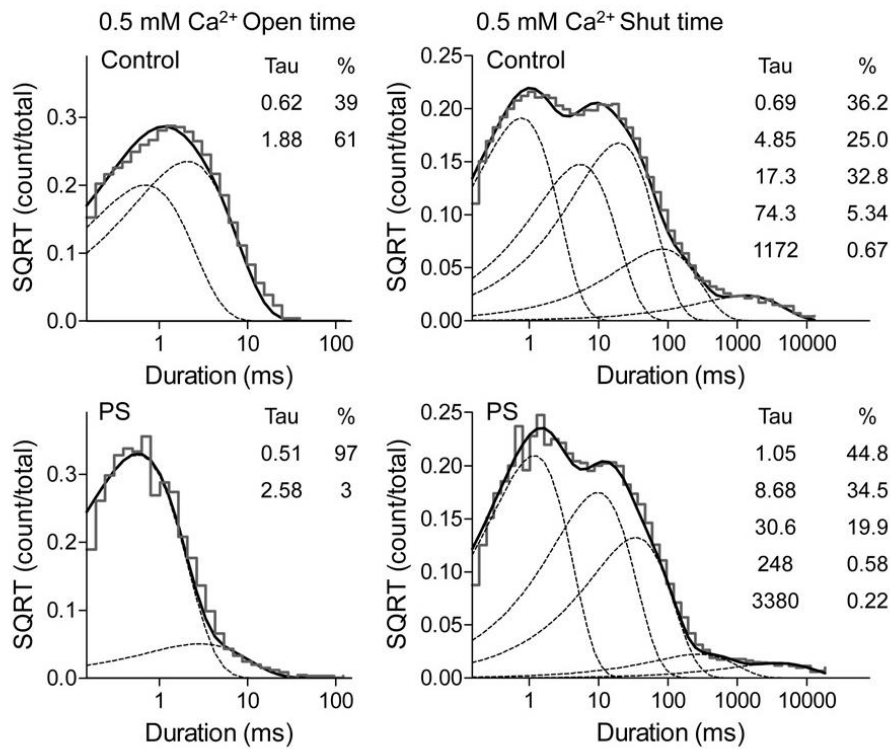


Figure 6: Inhibitory effect of pregnenolone sulfate on GluN1/GluN2A receptors is primarily due to reduced dwell-time in a longer open state.

Global dwell-time histograms were generated by summation of idealized data from individual cell-attached patches in the presence of 0.5 mM extracellular Ca²⁺. The open time histogram was fitted by a sum of two exponential components: control, 57,406 open events (n=5); PS, 85,892 events (n=6). The time constants and % area are shown in the inset. The dwell times from each patch were individually fitted and are presented in Table 1. PS was found to significantly increase the area of τ_1 and reduce the area of τ_2 with no change in the time constants themselves (Table 1). The composite shut time histogram was fitted by a sum of five exponential functions: control, 57,824 closed periods (n=5); PS, 85,903 closed periods (n=6). PS was found to significantly increase τ_1 but not other time constants or areas of the components (Table 1).

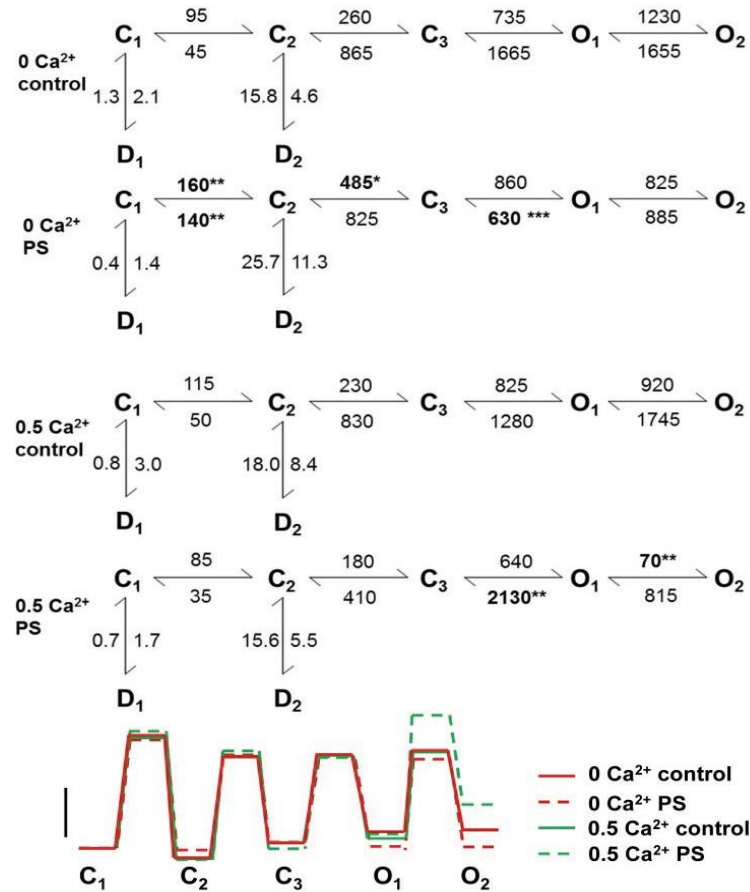


Figure 7: Kinetic mechanism describing the effects of pregnenolone sulfate on GluN1/GluN2A receptor activation.

MIL fit of single-channel data to understand the kinetic mechanism of GluN1/GluN2A receptor modulation by PS is shown. All rates are in sec^{-1} . Bold numbers with asterisks denote the rates which were significantly different from glutamate/glycine control patches. Rates \pm SEM are presented in Table 2. Data was analyzed using unpaired t -test. *** denotes $P < 0.001$, ** denotes $P < 0.01$, * denotes $P < 0.05$. Free-energy trajectories for the kinetic states in the different models are presented. Control with 0.5 mM Ca^{2+} or without nominal Ca^{2+} produced similar profiles. The free energies of the active open states are most dramatically affected by PS during either inhibition or potentiation of the receptor. Scale bar represents 1 k_BT.

H. TABLES

Table 1: Time constants and areas of closed and open components obtained from exponential fits.

Comparison of the time constants (τ , in ms) and relative contribution (a, % area of the component) of the open time and shut time components obtained from individual fits to the cell-attached patches. Data are mean \pm SEM. The values were compared by unpaired *t*-test.

*** indicates $p < 0.001$, ** indicates $p < 0.01$ and * indicates $p < 0.05$.

Time constants (ms) and areas (%)	0 Calcium		0.5 Calcium	
	Control (N=9)	PS (N=5)	Control (N=5)	PS (N=6)
Open time				
τ_1	0.31 \pm 0.04	0.86 \pm 0.27*	0.39 \pm 0.09	0.50 \pm 0.04
τ_2	1.76 \pm 0.26	3.62 \pm 0.37**	1.70 \pm 0.21	2.30 \pm 0.61
a1	22 \pm 4	25 \pm 8	22 \pm 7	87 \pm 5***
a2	78 \pm 4	75 \pm 8	78 \pm 7	13 \pm 5***
Shut time				
τ_1	0.63 \pm 0.04	0.63 \pm 0.16	0.69 \pm 0.12	1.03 \pm 0.09*
τ_2	5.80 \pm 0.43	2.93 \pm 0.53**	5.50 \pm 1.08	6.70 \pm 0.79
τ_3	19.3 \pm 1.2	12.4 \pm 1.3**	18.7 \pm 3.5	21.3 \pm 2.4
τ_4	73.6 \pm 8.8	50.4 \pm 10.1	90.0 \pm 34.6	117.0 \pm 47.9
τ_5	1117 \pm 198	3249 \pm 759*	1406 \pm 227	2176 \pm 628
a1	30 \pm 4	33 \pm 7	37 \pm 4	41 \pm 3
a2	27 \pm 1	31 \pm 4	24 \pm 3	28 \pm 4
a3	37 \pm 2	32 \pm 5	32 \pm 5	27 \pm 2
a4	4 \pm 1	4 \pm 2	7 \pm 2	4 \pm 2
a5	0.6 \pm 0.1	0.2 \pm 0.04*	0.5 \pm 0.1	0.4 \pm 0.1

Table 2: Hidden Markov maximum interval likelihood fitting of the steady state currents.

Idealized current records were fitted to the gating scheme as described in Figure 7. All rates have units of s^{-1} . Data are mean \pm SEM from patches containing one active channel fitted individually. The rates were compared by unpaired *t*-test. *** indicates $p<0.001$, ** indicates $p<0.01$ and * indicates $p<0.05$.

Rates (s^{-1})	0 Calcium		0.5 Calcium	
	Control N=9	PS N=5	Control N=5	PS N=6
$C_1 \rightarrow C_2$	95 \pm 5	160 \pm 20**	115 \pm 30	85 \pm 15
$C_2 \rightarrow C_1$	45 \pm 5	140 \pm 40**	50 \pm 15	35 \pm 5
$C_2 \rightarrow C_3$	260 \pm 10	485 \pm 120*	230 \pm 35	180 \pm 15
$C_3 \rightarrow C_2$	865 \pm 90	825 \pm 190	830 \pm 220	410 \pm 40
$C_3 \rightarrow O_1$	735 \pm 60	860 \pm 140	825 \pm 115	640 \pm 75
$O_1 \rightarrow C_3$	1665 \pm 150	630 \pm 80***	1280 \pm 135	2130 \pm 220**
$O_1 \rightarrow O_2$	1230 \pm 340	825 \pm 515	920 \pm 230	70 \pm 30**
$O_2 \rightarrow O_1$	1655 \pm 280	885 \pm 230	1745 \pm 480	815 \pm 290
$C_1 \rightarrow D_1$	2.1 \pm 0.4	1.4 \pm 0.3	3.0 \pm 1.4	1.7 \pm 0.5
$D_1 \rightarrow C_1$	1.3 \pm 0.3	0.4 \pm 0.1	0.8 \pm 0.2	0.7 \pm 0.2
$C_2 \rightarrow D_2$	4.6 \pm 1.2	11.3 \pm 4.4	8.4 \pm 1.9	5.5 \pm 2.0
$D_2 \rightarrow C_2$	15.8 \pm 1.5	25.7 \pm 6.3	18.0 \pm 4.2	15.6 \pm 4.0

I. REFERENCES

Chapter 1

Abele R, Keinanen K, and Madden DR (2000) Agonist-induced isomerization in a glutamate receptor ligand-binding domain. A kinetic and mutagenetic analysis. *J Biol Chem* **275**:21355–63.

Addy C, Assaid C, Hreniuk D, Stroh M, Xu Y, Herring WJ, Ellenbogen A, Jinnah HA, Kirby L, Leibowitz MT, Stewart RM, Tarsy D, Tetrud J, Stoch SA, Gottesdiener K, and Wagner J (2009) Single-dose administration of MK-0657, an NR2B-selective NMDA antagonist, does not result in clinically meaningful improvement in motor function in patients with moderate Parkinson's disease. *J Clin Pharmacol* **49**:856–64.

Albers GW, Goldstein LB, Hall D, and Lesko LM (2001) Aptiganel hydrochloride in acute ischemic stroke: a randomized controlled trial. *JAMA* **286**:2673–82.

Armstrong N, and Gouaux E (2000) Mechanisms for activation and antagonism of an AMPA-sensitive glutamate receptor: crystal structures of the GluR2 ligand binding core. *Neuron* **28**:165–81.

Auerbach A, and Zhou Y (2005) Gating reaction mechanisms for NMDA receptor channels. *J Neurosci* **25**:7914–23.

Banke TG, Dravid SM, and Traynelis SF (2005) Protons trap NR1/NR2B NMDA receptors in a nonconducting state. *J Neurosci* **25**:42–51.

Banke TG, and Traynelis SF (2003) Activation of NR1/NR2B NMDA receptors. *Nat Neurosci* **6**:144–52.

Baulieu EE, Robel P, and Schumacher M (2001) Neurosteroids: beginning of the story. *Int Rev Neurobiol* **46**:1–32.

Bébé P, Stern P, Wyllie DJ, Nassar M, Schoepfer R, and Colquhoun D (1995) Determination of NMDA NR1 subunit copy number in recombinant NMDA receptors. *Proc Biol Sci* **262**:205–13.

Bhatt JM, Prakash A, Suryavanshi PS, and Dravid SM (2013) Effect of ifenprodil on GluN1/GluN2B N-methyl-D-aspartate receptor gating. *Mol Pharmacol* **83**:9–21.

Blahos J, and Wenthold RJ (1996) Relationship between N-methyl-D-aspartate receptor NR1 splice variants and NR2 subunits. *J Biol Chem* **271**:15669–74.

Blanpied TA, Boeckman FA, Aizenman E, and Johnson JW (1997) Trapping channel block of NMDA-activated responses by amantadine and memantine. *J Neurophysiol* **77**:309–23.

Burzomato V, Beato M, Groot-Kormelink PJ, Colquhoun D, and Sivilotti LG (2004) Single-channel behavior of heteromeric alpha1beta glycine receptors: an attempt to detect a conformational change before the channel opens. *J Neurosci* **24**:10924–40.

Castillo PE, Malenka RC, and Nicoll RA (1997) Kainate receptors mediate a slow postsynaptic current in hippocampal CA3 neurons. *Nature* **388**:182–6.

Ceccon M, Rumbaugh G, and Vicini S (2001) Distinct effect of pregnenolone sulfate on NMDA receptor subtypes. *Neuropharmacology* **40**:491–500.

Chen HS, and Lipton SA (1997) Mechanism of memantine block of NMDA-activated channels in rat retinal ganglion cells: uncompetitive antagonism. *J Physiol* **499** (Pt 1:27–46.

Chen H-SV, and Lipton SA (2006) The chemical biology of clinically tolerated NMDA receptor antagonists. *J Neurochem* **97**:1611–26.

Cheng Q, Du M, Ramanoudjame G, and Jayaraman V (2005) Evolution of glutamate interactions during binding to a glutamate receptor. *Nat Chem Biol* **1**:329–32.

Choi YB, and Lipton SA (1999) Identification and mechanism of action of two histidine residues underlying high-affinity Zn²⁺ inhibition of the NMDA receptor. *Neuron* **23**:171–80.

Collingridge GL, Isaac JTR, and Wang YT (2004) Receptor trafficking and synaptic plasticity. *Nat Rev Neurosci* **5**:952–62.

Collingridge GL, Volianskis A, Bannister N, France G, Hanna L, Mercier M, Tidball P, Fang G, Irvine MW, Costa BM, Monaghan DT, Bortolotto ZA, Molnár E,

Lodge D, and Jane DE (2013) The NMDA receptor as a target for cognitive enhancement. *Neuropharmacology* **64**:13–26.

Crosby N, Deane KH, and Clarke CE (2003) Amantadine in Parkinson's disease. *Cochrane database Syst Rev* CD003468.

Cull-Candy S, Brickley S, and Farrant M (2001) NMDA receptor subunits: diversity, development and disease. *Curr Opin Neurobiol* **11**:327–35.

Dang K, Naeem S, Walker K, Bowery NG, and Urban L (2002) Interaction of group I mGlu and NMDA receptor agonists within the dorsal horn of the spinal cord of the juvenile rat. *Br J Pharmacol* **136**:248–54.

Dravid SM, Erreger K, Yuan H, Nicholson K, Le P, Lyuboslavsky P, Almonte A, Murray E, Mosely C, Barber J, French A, Balster R, Murray TF, and Traynelis SF (2007) Subunit-specific mechanisms and proton sensitivity of NMDA receptor channel block. *J Physiol* **581**:107–28.

Erreger K, Dravid SM, Banke TG, Wyllie DJA, and Traynelis SF (2005) Subunit-specific gating controls rat NR1/NR2A and NR1/NR2B NMDA channel kinetics and synaptic signalling profiles. *J Physiol* **563**:345–58.

Frederickson CJ (1989) Neurobiology of zinc and zinc-containing neurons. *Int Rev Neurobiol* **31**:145–238.

Furukawa H, Singh SK, Mancusso R, and Gouaux E (2005) Subunit arrangement and function in NMDA receptors. *Nature* **438**:185–92.

Gibb AJ, and Colquhoun D (1991) Glutamate activation of a single NMDA receptor-channel produces a cluster of channel openings. *Proc Biol Sci* **243**:39–45.

Gielen M, Retchless BS, Mony L, Johnson JW, and Paoletti P (2009) Mechanism of differential control of NMDA receptor activity by NR2 subunits. *Nature* **459**:703–707.

Green AR (2002) Why do neuroprotective drugs that are so promising in animals fail in the clinic? An industry perspective. *Clin Exp Pharmacol Physiol* **29**:1030–4.

Hallett PJ, and Standaert DG (2004) Rationale for and use of NMDA receptor antagonists in Parkinson's disease. *Pharmacol Ther* **102**:155–74.

Hardingham GE, and Bading H (2003) The Yin and Yang of NMDA receptor signalling. *Trends Neurosci* **26**:81–9.

Hedegaard M, Hansen KB, Andersen KT, Bräuner-Osborne H, and Traynelis SF (2012) Molecular pharmacology of human NMDA receptors. *Neurochem Int* **61**:601–9.

Heresco-Levy U, Kremer I, Javitt DC, Goichman R, Reshef A, Blanaru M, and Cohen T (2002) Pilot-controlled trial of D-cycloserine for the treatment of post-traumatic stress disorder. *Int J Neuropsychopharmacol* **5**:301–7.

Hofmann SG, Meuret AE, Smits JAJ, Simon NM, Pollack MH, Eisenmenger K, Shiekh M, and Otto MW (2006) Augmentation of exposure therapy with D-cycloserine for social anxiety disorder. *Arch Gen Psychiatry* **63**:298–304.

Horak M, Vlcek K, Chodounska H, and Vyklicky L (2006) Subtype-dependence of N-methyl-D-aspartate receptor modulation by pregnenolone sulfate. *Neuroscience* **137**:93–102.

Horak M, Vlcek K, Petrovic M, Chodounska H, and Vyklicky L (2004) Molecular mechanism of pregnenolone sulfate action at NR1/NR2B receptors. *J Neurosci* **24**:10318–25.

Ikonomidou C, and Turski L (2002) Why did NMDA receptor antagonists fail clinical trials for stroke and traumatic brain injury? *Lancet Neurol* **1**:383–6.

Jahr CE, and Stevens CF (1993) Calcium permeability of the N-methyl-D-aspartate receptor channel in hippocampal neurons in culture. *Proc Natl Acad Sci U S A* **90**:11573–7.

Jang M-K, Mierke DF, Russek SJ, and Farb DH (2004) A steroid modulatory domain on NR2B controls N-methyl-D-aspartate receptor proton sensitivity. *Proc Natl Acad Sci U S A* **101**:8198–203.

Johnson JW, and Ascher P Glycine potentiates the NMDA response in cultured mouse brain neurons. *Nature* **325**:529–31.

Kalia L V, Kalia SK, and Salter MW (2008) NMDA receptors in clinical neurology: excitatory times ahead. *Lancet Neurol* **7**:742–55.

Karakas E, Simorowski N, and Furukawa H (2011) Subunit arrangement and phenylethanolamine binding in GluN1/GluN2B NMDA receptors. *Nature* **475**:249–53.

Kemp JA, and McKernan RM (2002) NMDA receptor pathways as drug targets. *Nat Neurosci* **5 Suppl**:1039–42.

Kerchner GA, and Nicoll RA (2008) Silent synapses and the emergence of a postsynaptic mechanism for LTP. *Nat Rev Neurosci* **9**:813–25.

Kleckner NW, and Dingledine R (1988) Requirement for glycine in activation of NMDA-receptors expressed in *Xenopus* oocytes. *Science* **241**:835–7.

Kostakis E, Jang M-K, Russek SJ, Gibbs TT, and Farb DH (2011) A steroid modulatory domain in NR2A collaborates with NR1 exon-5 to control NMDAR modulation by pregnenolone sulfate and protons. *J Neurochem* **119**:486–96.

Kotermanski SE, Wood JT, and Johnson JW (2009) Memantine binding to a superficial site on NMDA receptors contributes to partial trapping. *J Physiol* **587**:4589–604.

Krystal JH, Anand A, and Moghaddam B (2002) Effects of NMDA receptor antagonists: implications for the pathophysiology of schizophrenia. *Arch Gen Psychiatry* **59**:663–4.

Langmead CJ, and Christopoulos A (2006) Allosteric agonists of 7TM receptors: expanding the pharmacological toolbox. *Trends Pharmacol Sci* **27**:475–81.

Lau CG, and Zukin RS (2007) NMDA receptor trafficking in synaptic plasticity and neuropsychiatric disorders. *Nat Rev Neurosci* **8**:413–26.

Lipton SA, and Rosenberg PA (1994) Excitatory amino acids as a final common pathway for neurologic disorders. *N Engl J Med* **330**:613–22.

Malayev A, Gibbs TT, and Farb DH (2002) Inhibition of the NMDA response by pregnenolone sulphate reveals subtype selective modulation of NMDA receptors by sulphated steroids. *Br J Pharmacol* **135**:901–9.

McBain CJ, and Mayer ML (1994) N-methyl-D-aspartic acid receptor structure and function. *Physiol Rev* **74**:723–60.

Mealing GA, Lanthorn TH, Murray CL, Small DL, and Morley P (1999) Differences in degree of trapping of low-affinity uncompetitive N-methyl-D-aspartic acid receptor antagonists with similar kinetics of block. *J Pharmacol Exp Ther* **288**:204–10.

Meddows E, Le Bourdelles B, Grimwood S, Wafford K, Sandhu S, Whiting P, and McIlhinney RA (2001) Identification of molecular determinants that are important in the assembly of N-methyl-D-aspartate receptors. *J Biol Chem* **276**:18795–803.

Möbius HJ, and Stöffler A (2003) Memantine in vascular dementia. *Int Psychogeriatr* **15 Suppl 1**:207–13.

Moriyoshi K, Masu M, Ishii T, Shigemoto R, Mizuno N, and Nakanishi S (1991) Molecular cloning and characterization of the rat NMDA receptor. *Nature* **354**:31–7.

Muir KW (2006) Glutamate-based therapeutic approaches: clinical trials with NMDA antagonists. *Curr Opin Pharmacol* **6**:53–60.

Mullasseril P, Hansen KB, Vance KM, Ogden KK, Yuan H, Kurtkaya NL, Santangelo R, Orr AG, Le P, Vellano KM, Liotta DC, and Traynelis SF (2010) A subunit-selective potentiator of NR2C- and NR2D-containing NMDA receptors. *Nat Commun* **1**:90.

Paoletti P (2011) Molecular basis of NMDA receptor functional diversity. *Eur J Neurosci* **33**:1351–1365.

Paoletti P, Bellone C, and Zhou Q (2013) NMDA receptor subunit diversity: impact on receptor properties, synaptic plasticity and disease. *Nat Rev Neurosci* **14**:383–400.

Paoletti P, and Neyton J (2007) NMDA receptor subunits: function and pharmacology. *Curr Opin Pharmacol* **7**:39–47.

Paoletti P, Vergnano AM, Barbour B, and Casado M (2009) Zinc at glutamatergic synapses. *Neuroscience* **158**:126–36.

Park-Chung M, Wu FS, Purdy RH, Malayev AA, Gibbs TT, and Farb DH (1997) Distinct sites for inverse modulation of N-methyl-D-aspartate receptors by sulfated steroids. *Mol Pharmacol* **52**:1113–23.

Parsons CG, Quack G, Bresink I, Baran L, Przegalinski E, Kostowski W, Krzascik P, Hartmann S, and Danysz W (1995) Comparison of the potency, kinetics and voltage-dependency of a series of uncompetitive NMDA receptor antagonists in vitro with anticonvulsive and motor impairment activity in vivo. *Neuropharmacology* **34**:1239–58.

Premkumar LS, and Auerbach A (1996) Identification of a high affinity divalent cation binding site near the entrance of the NMDA receptor channel. *Neuron* **16**:869–80.

Pullan LM, Olney JW, Price MT, Compton RP, Hood WF, Michel J, and Monahan JB (1987) Excitatory amino acid receptor potency and subclass specificity of sulfur-containing amino acids. *J Neurochem* **49**:1301–7.

Santangelo RM, Acker TM, Zimmerman SS, Katzman BM, Strong KL, Traynelis SF, and Liotta DC (2012) Novel NMDA receptor modulators: an update. *Expert Opin Ther Pat* **22**:1337–52.

Schmitt A, Fendt M, Zink M, Ebert U, Starke M, Berthold M, Herb A, Petroianu G, Falkai P, and Henn FA (2007) Altered NMDA receptor expression and behavior following postnatal hypoxia: potential relevance to schizophrenia. *J Neural Transm* **114**:239–48.

Schorge S, Elenes S, and Colquhoun D (2005) Maximum likelihood fitting of single channel NMDA activity with a mechanism composed of independent dimers of subunits. *J Physiol* **569**:395–418.

Schumacher M, Liere P, Akwa Y, Rajkowski K, Griffiths W, Bodin K, Sjövall J, and Baulieu E-E Pregnenolone sulfate in the brain: a controversial neurosteroid. *Neurochem Int* **52**:522–40.

Sharma G, and Stevens CF (1996) Interactions between two divalent ion binding sites in N-methyl-D-aspartate receptor channels. *Proc Natl Acad Sci U S A* **93**:14170–5.

Shleper M, Kartvelishvily E, and Wolosker H (2005) D-serine is the dominant endogenous coagonist for NMDA receptor neurotoxicity in organotypic hippocampal slices. *J Neurosci* **25**:9413–7.

Skolnick P, Popik P, and Trullas R (2009) Glutamate-based antidepressants: 20 years on. *Trends Pharmacol Sci* **30**:563–9.

Sobolevsky AI, Rosconi MP, and Gouaux E (2009) X-ray structure, symmetry and mechanism of an AMPA-subtype glutamate receptor. *Nature* **462**:745–56.

Tang YP, Shimizu E, Dube GR, Rampon C, Kerchner GA, Zhuo M, Liu G, and Tsien JZ (1999) Genetic enhancement of learning and memory in mice. *Nature* **401**:63–9.

Tariot PN (2006) Contemporary issues in the treatment of Alzheimer's disease: tangible benefits of current therapies. *J Clin Psychiatry* **67 Suppl 3**:15–22; quiz 23.

Traynelis SF, Burgess MF, Zheng F, Lyuboslavsky P, and Powers JL (1998) Control of voltage-independent zinc inhibition of NMDA receptors by the NR1 subunit. *J Neurosci* **18**:6163–75.

Traynelis SF, Wollmuth LP, McBain CJ, Menniti FS, Vance KM, Ogden KK, Hansen KB, Yuan H, Myers SJ, and Dingledine R (2010) Glutamate receptor ion channels: structure, regulation, and function. *Pharmacol Rev* **62**:405–96.

Tsai G, and Coyle JT (2002) Glutamatergic mechanisms in schizophrenia. *Annu Rev Pharmacol Toxicol* **42**:165–79.

Watanabe J, Beck C, Kuner T, Premkumar LS, and Wollmuth LP (2002) DRPEER: a motif in the extracellular vestibule conferring high Ca²⁺ flux rates in NMDA receptor channels. *J Neurosci* **22**:10209–16.

Winblad B, Jones RW, Wirth Y, Stöffler A, and Möbius HJ (2007) Memantine in moderate to severe Alzheimer's disease: a meta-analysis of randomised clinical trials. *Dement Geriatr Cogn Disord* **24**:20–7.

Wollmuth LP, and Sobolevsky AI (2004) Structure and gating of the glutamate receptor ion channel. *Trends Neurosci* **27**:321–8.

Wu FS, Gibbs TT, and Farb DH (1991) Pregnenolone sulfate: a positive allosteric modulator at the N-methyl-D-aspartate receptor. *Mol Pharmacol* **40**:333–6.

Yuan H, Erreger K, Dravid SM, and Traynelis SF (2005) Conserved structural and functional control of N-methyl-D-aspartate receptor gating by transmembrane domain M3. *J Biol Chem* **280**:29708–16.

Yuan H, Hansen KB, Vance KM, Ogden KK, and Traynelis SF (2009) Control of NMDA receptor function by the NR2 subunit amino-terminal domain. *J Neurosci* **29**:12045–58.

Zuo J, De Jager PL, Takahashi KA, Jiang W, Linden DJ, and Heintz N (1997) Neurodegeneration in Lurcher mice caused by mutation in delta2 glutamate receptor gene. *Nature* **388**:769–73.

Chapter2

Acker TM, Yuan H, Hansen KB, Vance KM, Ogden KK, Jensen HS, Burger PB, Mullasseril P, Snyder JP, Liotta DC and Traynelis SF (2011) Mechanism for noncompetitive inhibition by novel GluN2C/D N-methyl-D-aspartate receptor subunit-selective modulators. *Mol Pharmacol* **80**:782-795.

Banke TG and Traynelis SF (2003) Activation of NR1/NR2B NMDA receptors. *Nat Neurosci* **6**:144-152.

Bhatt JM, Prakash A, Suryavanshi PS and Dravid SM (2013) Effect of ifenprodil on GluN1/GluN2B N-methyl-D-aspartate receptor gating. *Mol Pharmacol* **83**:9-21.

Borovska J, Vyklicky V, Stastna E, Kapras V, Slavikova B, Horak M, Choudounska H and Vyklicky L, Jr (2012) Access of inhibitory neurosteroids to the NMDA receptor. *Br J Pharmacol* **166**:1069-1083.

Bowlby MR (1993) Pregnenolone sulfate potentiation of N-methyl-D-aspartate receptor channels in hippocampal neurons. *Mol Pharmacol* **43**:813-819.

Cameron K, Bartle E, Roark R, Fanelli D, Pham M, Pollard B, Borkowski B, Rhoads S, Kim J, Rocha M, Kahlson M, Kangala M and Gentile L (2012) Neurosteroid binding to the

amino terminal and glutamate binding domains of ionotropic glutamate receptors. *Steroids* **77**:774-779.

Ceccon M, Rumbaugh G and Vicini S (2001) Distinct effect of pregnenolone sulfate on NMDA receptor subtypes. *Neuropharmacology* **40**:491-500.

Dravid SM, Prakash A and Traynelis SF (2008) Activation of recombinant NR1/NR2C NMDA receptors. *J Physiol* **586**:4425-4439.

Erreger K, Dravid SM, Banke TG, Wyllie DJ and Traynelis SF (2005) Subunit-specific gating controls rat NR1/NR2A and NR1/NR2B NMDA channel kinetics and synaptic signalling profiles. *J Physiol* **563**:345-358.

Hedegaard M, Hansen KB, Andersen KT, Brauner-Osborne H and Traynelis SF (2012) Molecular pharmacology of human NMDA receptors. *Neurochem Int* **61**:601-609.

Horak M, Vlcek K, Chodounska H and Vyklicky L (2006) Subtype-dependence of N-methyl-d-aspartate receptor modulation by pregnenolone sulfate. *Neuroscience* **137**:93-102.

Horak M, Vlcek K, Petrovic M, Chodounska H and Vyklicky L, Jr (2004) Molecular mechanism of pregnenolone sulfate action at NR1/NR2B receptors. *J Neurosci* **24**:10318-10325.

Jahr CE and Stevens CF (1993) Calcium permeability of the N-methyl-D-aspartate receptor channel in hippocampal neurons in culture. *Proc Natl Acad Sci U S A* **90**:11573-11577.

Jang MK, Mierke DF, Russek SJ and Farb DH (2004) A steroid modulatory domain on NR2B controls N-methyl-D-aspartate receptor proton sensitivity. *Proc Natl Acad Sci U S A* **101**:8198-8203.

Karakas E and Furukawa H (2014) Crystal structure of a heterotetrameric NMDA receptor ion channel *Science* **344**:992-997.

Kostakis E, Jang MK, Russek SJ, Gibbs TT and Farb DH (2011) A steroid modulatory domain in NR2A collaborates with NR1 exon-5 to control NMDAR modulation by pregnenolone sulfate and protons. *J Neurochem* **119**:486-496.

Kussius CL and Popescu GK (2009) Kinetic basis of partial agonism at NMDA receptors. *Nat Neurosci* **12**:1114-1120.

Malayev A, Gibbs TT and Farb DH (2002) Inhibition of the NMDA response by pregnenolone sulphate reveals subtype selective modulation of NMDA receptors by sulphated steroids. *Br J Pharmacol* **135**:901 <last_page> 909.

Marx CE, Lee J, Subramaniam M, Rapisarda A, Bautista DCT, Chan E, Kilts JD, Buchanan RW, Wai EP, Verma S, Sim K, Hariram J, Jacob R, Keefe RSE and Chong SA (2014; 2014) Proof-of-concept randomized controlled trial of pregnenolone in schizophrenia. *Psychopharmacology (Berl)* **231**:3647 <last_page> 3662.

Murthy SE, Shogan T, Page JC, Kasperek EM and Popescu GK (2012) Probing the activation sequence of NMDA receptors with lurcher mutations. *J Gen Physiol* **140**:267-277.

Park-Chung M, Wu FS, Purdy RH, Malayev AA, Gibbs TT and Farb DH (1997) Distinct sites for inverse modulation of N-methyl-D-aspartate receptors by sulfated steroids. *Mol Pharmacol* **52**:1113-1123.

Petrovic M, Sedlacek M, Cais O, Horak M, Chodounska H and Vyklicky L, Jr (2009) Pregnenolone sulfate modulation of N-methyl-D-aspartate receptors is phosphorylation dependent. *Neuroscience* **160**:616-628.

Qin F, Auerbach A and Sachs F (1996) Estimating single-channel kinetic parameters from idealized patch-clamp data containing missed events. *Biophys J* **70**:264-280.

Robel P and Baulieu E (1994) Neurosteroids. *Trends in Endocrinology & Metabolism* **5**:1 <last_page> 8.

Sather W, Johnson JW, Henderson G and Ascher P (1990) Glycine-insensitive desensitization of NMDA responses in cultured mouse embryonic neurons *Neuron* **4**:725-731.

Schorge S, Elenes S and Colquhoun D (2005) Maximum likelihood fitting of single channel NMDA activity with a mechanism composed of independent dimers of subunits *J Physiol* **569**:395-418.

Sullivan JM, Traynelis SF, Chen HS, Escobar W, Heinemann SF and Lipton SA (1994) Identification of two cysteine residues that are required for redox modulation of the NMDA subtype of glutamate receptor *Neuron* **13**:929-936.

Talukder I and Wollmuth LP (2011) Local constrains in either the GluN1 or GluN2 subunit equally impair NMDA receptor pore opening *J Gen Physiol* **138**:179-194.

Traynelis SF, Wollmuth LP, McBain CJ, Menniti FS, Vance KM, Ogden KK, Hansen KB, Yuan H, Myers SJ and Dingledine R (2010) Glutamate receptor ion channels: structure, regulation, and function. *Pharmacol Rev* **62**:405-496.

Watanabe J, Beck C, Kuner T, Premkumar LS and Wollmuth LP (2002) DRPEER: a motif in the extracellular vestibule conferring high Ca²⁺ flux rates in NMDA receptor channels. *J Neurosci* **22**:10209-10216.

Wong P, Sze Y, Chang CC, Lee J and Zhang X (2015) Pregnenolone sulfate normalizes schizophrenia-like behaviors in dopamine transporter knockout mice through the AKT/GSK3beta pathway. *Transl Psychiatry* **5**:e528.

Wu FS, Gibbs TT and Farb DH (1991) Pregnenolone sulfate: a positive allosteric modulator at the N-methyl-D-aspartate receptor. *Mol Pharmacol* **40**:333-336.

Yaghoubi N, Malayev A, Russek SJ, Gibbs TT and Farb DH (1998) Neurosteroid modulation of recombinant ionotropic glutamate receptors. *Brain Res* **803**:153-160.

Chapter 3

**Stabilization of closed glutamate-binding domain
as a gating mechanism of a novel GluN1/GluN2A
receptor potentiator**

A. ABSTRACT:

NMDA receptors are gated by binding of glycine and glutamate to GluN1 and GluN2 subunits respectively. Although gating mechanism of several negative allosteric modulators of NMDA receptors such as zinc, ifenprodil and pregnenolone sulfate are well understood, the mechanisms of newly discovered potentiators are still poorly understood. We tested the effect of a novel pan-potentiator which increases the function of NMDA receptor at all GluN2 subunits. We found that at GluN1/GluN2A receptors heterologously expressed in HEK293 UBP684 lead to potentiation of peak current in perforated whole-cell recordings conditions, however, the potentiation was lost in dialyzed conditions. UBP684 also slowed the deactivation of GluN1/GluN2A receptors irrespective of whole-cell condition. Single channel analysis revealed a robust effect of UBP684 both on mean open time which was significantly increased and mean shut time which was significantly reduced. In order to determine potential mechanism of action of UBP684 we compared the shut time histogram as a signature to identify mutants or agents that produce similar effects. We found that the effect of UBP684 on shut times had similarity to those produced by locking of ligand-binding domains in closed clamshell conformation and that produced by redox modulation by DTT. We propose that UBP684 increases the efficacy of opening of the receptor by stabilizing closure of the ligand-binding domain.

B. INTRODUCTION:

NMDA receptors (NMDARs) are one of the major ionotropic glutamate receptors at central synapses composed of two GluN1 and two GluN2 subunits and are gated by binding of glycine or D-serine to GluN1 subunit and glutamate to GluN2 subunit. Activation of NMDARs lead to influx of Ca^{2+} which through second messenger mechanisms leads to synaptic plasticity and during excessive activation produces neuronal death. Development of drugs acting at NMDARs has not been able to fully translate into clinical setting due to unwanted side effects. Initial discoveries primarily focused on the development of competitive agents and channel-blockers although some allosteric modulators particularly those acting selectively at GluN2B-containing receptors have been pursued. Use of allosteric modulators provides the ability to fine tune the receptor response, which is not achievable with competitive agents. Allosteric agents may also act at less conserved sites, and hence there are better chances of achieving subtype-selectivity. Development of positive allosteric modulators for NMDARs has gained significant interest (Ogden et al., 2011) since NMDAR potentiation is proposed to be useful in treating cognitive deficits such as those observed in schizophrenia and autism. Recent drug discovery efforts have identified novel allosteric modulators which can potentiate or inhibit NMDARs with some having unique subunit-selectivities and may serve as promising lead compounds. However, the mechanism of action of these modulators remains poorly understood. We tested the effect of a novel positive allosteric modulator (PAM) UBP684 which is from the phenanthrene and naphthalene derivatives family on NMDAR function

using whole-cell and single-channel studies on oocytes and HEK293 cells in order to gain a better understanding of their gating kinetics and mechanism of action at GluN1/GluN2A receptors. We also utilized previously known changes in gating mechanisms by mutational analysis to predict the conformational change induced by UBP684. Our studies identify a mechanism whereby UBP684 stabilizes a receptor conformation where the ligand-binding domain is in a locked closed conformation.

C. MATERIALS AND METHODS:

Expression of recombinant NMDARs: Human embryonic kidney (HEK) 293 cells were maintained as previously described (Dravid et al., 2008). The cells were transiently transfected with GluN1 and GluN2A subunits and green fluorescent protein (GFP) in the ratio of 1:2:0.5 were used as previously described using Viafect™ reagent (Promega Corporation, Madison, WI) as previously described (Chopra et al., 2015). Mutants having cysteine substitutions at N499C and Q686C in GluN1 (GluN1^c) and for K487C and N687C in GluN2A (GluN2A^c) (provided by Dr. Gabriela Popescu). Electrophysiology experiments were performed 16–48 hours after transfection.

Electrophysiology: Electrophysiological recordings in whole-cell and single-channel mode were obtained from transfected HEK 293 cells at room temperature (22–25°C). An external solution containing (in mM) 150 NaCl, 3 KCl, 10 HEPES, 0.5 CaCl₂ and 6 mannitol (to adjust osmolarity) was used for the recordings unless otherwise stated. Recordings were conducted in the absence of nominal extracellular CaCl₂. The external pH was adjusted to 7.4 with NaOH. This solution was supplemented with 0.02 mM EDTA to chelate trace amounts of zinc. The same external solution was used for whole-cell

recordings, as well as cell-attached recordings. Recordings were performed under two conditions: (1) 100 μ M glutamate, 100 μ M glycine (control patches); and (2) 100 μ M glutamate, 100 μ M glycine and 100 μ M UBP684. For whole-cell recordings, agonists and UBP684 were added to the extracellular solution, and for cell-attached recordings, these drugs were present only in the pipette solution. Recordings were obtained using a Axopatch 200B amplifier (Axon Instruments/Molecular Devices) and digitized with pCLAMP 10 software (Axon Instruments/Molecular Devices). Whole-cell recordings were obtained at -70 mV, filtered at 2 kHz, and digitized at 5 kHz. For cell-attached recordings a potential (V_m) of +70 mV was applied and data were filtered at 5 kHz (-3 dB, 8-pole Bessel) and digitized at 20 kHz. Single-channel amplitude was not corrected for junction potential.

The internal solution used for whole-cell recordings consisted of (in mM) 110 cesium gluconate, 30 CsCl₂, 5 HEPES, 4 NaCl, 0.5 CaCl₂, 2 MgCl₂, 5 BAPTA, 2 Na₂ATP, and 0.3 Na₂GTP (pH 7.3). For perforated whole-cell patch-clamp recordings 20 μ g/ml of gramicidin was added to the pipette internal solution. Whole-cell configuration after gigaohm seal was reached typically within 10-15 minutes. Rapid perfusion for whole-cell concentration jumps was achieved with a two-barreled theta glass pipette controlled by a piezoelectric translator (Burleigh). The solution exchange times for 10–90% solution were typically ~1-2 ms. Two concentration profiles were obtained: (1) 100 μ M glutamate, 100 μ M glycine, and (2) 100 μ M glutamate, 100 μ M glycine and 100 μ M UBP684. The cell was moved from the control solution with no drugs to a solution containing agonists \pm UBP684. Drug application was typically for 2.5 s during each 15 s sweep.

D. Data processing and kinetic modeling:

Recordings containing a single active channel were idealized using QUB software (www.qub.buffalo.edu) as previously described (Bhatt et al., 2013; Dravid et al., 2008). The idealized data was used for maximum interval likelihood fitting (MIL; Qin et al., 1996). A 120 μ s dead time was imposed using QUB. All gating steps were free and not constrained. The C5O2 model consisting of 3 closed and 2 open states in linear configuration and two desensitized states emerging from C1 and C2 respectively (Figure 7) provided the best fit to the single channel data based on the log likelihood values. Other models tested included a C4O2 model with four instead of five closed states and a model where the receptor can transition to either a fast or slow gating step as described previously (Bhatt et al., 2013). The mean open time, mean shut time and open probability was obtained from the idealized data using ChanneLab (www.synaptosoft.com), with an imposed dead time of 120 μ s. Peak and steady state responses and deactivation, and desensitization time course for whole-cell recordings were analyzed using Clampfit (pClamp 10.2).

Statistical Analysis: All the values are expressed as mean \pm SEM. Data were compared using paired *t*-test for macroscopic current profiles and unpaired *t*-test and one-way ANOVA for the cell-attached patches. Values of $P \leq 0.05$ were considered significantly different.

E. RESULTS:

Effect of UBP684 on macroscopic currents is dependent on intracellular milieu

We first determined the EC₅₀ of UBP684 in oocytes expressing GluN1/GluN2A subunits. UBP684 produced a potentiation of approximately 50-70% with a EC₅₀ of 15 μM. We tested the effect of UBP684 on macroscopic GluN1/GluN2A whole-cell currents under dialyzed (non-perforated) conditions. UBP684 (100 μM) was co-applied with glutamate (100 μM) and glycine (100 μM) (Figure 1). UBP684 produced no effect on the peak response (p=0.9327, N=6, paired t-test, $I_{\text{UBP684}}/I_{\text{control}}=0.996\pm0.077$) but slowed the deactivation kinetics from 103.08±27.63 ms in control condition to 163.53±41.58 ms (p=0.0226). We have recently shown that modulation of NMDAR responses by pregnenolone sulfate is affected by mode of whole-cell recording as has been previously described (Chopra et al., 2013; Acker et al., 2011; Petrovic et al., 2009). We performed perforated whole-cell recordings using gramicidin to test whether keeping intracellular milieu intact would affect UBP684 modulatory actions. In perforated patch mode UBP684 significantly increased the peak response by two-fold (p=0.0207, N=6, $I_{\text{UBP684}}/I_{\text{control}}=2.134\pm0.204$) and also slowed the deactivation from 95.293±21.31 ms to 156.62.53±36.54 ms (p=0.0206). A transient rise in current was observed in the whole-cell recordings when the solution containing UBP684 and agonists was washed-out which is also similar to effect produced by pregnenolone sulfate (Chopra et al., 2015). Thus the increase in deactivation kinetics and transient increase in current during wash-out was independent of the whole-cell mode.

UBP684 increases the open probability of the GluN1/GluN2A receptors

In order to determine the mechanism by which UBP684 exerts its potentiating effects we studied the effect of UBP684 on single-channel responses in cell-attached patch clamp mode which replicates gramicidin-perforated whole-cell mode as it will have minimal effect on intracellular milieu. We obtained cell-attached patches with one-active channel for evaluating the effect of UBP684 on GluN1/GluN2A gating (Figure 2). UBP684 produced a significant increase in the mean open time (\pm SEM) from 2.27 ± 0.28 ms (262,707 events; N=7) in control patches to 5.03 ± 0.77 ms (403,922 events; N=9, $p=0.0096$, unpaired *t*-test). The mean shut time was reduced by UBP684; 20.05 ± 2.92 ms in control patches (263,098 events) to 4.40 ± 0.54 ms in UBP684 patches (403,937 events, $p<0.001$). Consequently, the open probability, measured over the entire length of recordings, was found to increase from 0.135 ± 0.030 in control patches to 0.524 ± 0.033 in UBP684 patches ($p<0.001$). The amplitude of openings was unaffected by UBP684.

We further evaluated the effect of UBP684 on the open and shut time characteristics. Both control and UBP684 patches demonstrated reasonably good fits with a scheme with five shut states and two closed states as previously described (Dravid et al., 2008) suggesting this model provides a reasonable description of the receptor gating. These results demonstrate that UBP684 does not affect the number of kinetic states that the receptor traverses before opening. UBP684 increased the time constants for the open states (control, $\tau_1=0.31\pm 0.06$, $\tau_2=2.66\pm 0.35$; UBP684, $\tau_1=0.88\pm 0.18$ ($p=0.0201$), $\tau_2=5.90\pm 0.93$ ($p=0.0112$)). The shift in the open time constants is consistent with an increase in the mean open time observed in the presence of UBP684 (Figure 2). No significant change was observed in the areas of open states.

UBP684 produces dramatic changes in the shut times which resemble effects of locked closed conformation of GluN2 ligand-binding domain

Analysis of shut time constants revealed a dramatic shift in closed conformational states by UBP684. The time constants τ_2 , τ_3 were significantly different (Table 1). UBP684 caused a decrease in time constants τ_2 and τ_3 for shut states (control, $\tau_2=4.3711\pm 0.93$, $\tau_3=15.936\pm 5.73$; UBP684, $\tau_2=1.3738\pm 0.18$ ($p=0.0069$), $\tau_3=4.6319\pm 0.36$ ($p=0.0017$)). UBP684 also caused a reduction in the area of τ_3 shut time constant (control, $a_3=40.15\pm 3.95\%$; UBP684, $a_3=23.25\pm 3.95\%$ ($p=0.0098$)). The shift in the shut time constants is in accordance with a reduction in the mean shut time in the presence of UBP684 (Figure 2). Interestingly, such a dramatic shift in shut time has been observed previously by mutant receptors in which the LBD are covalently kept in a closed conformation by disulfide bridges of engineered cysteines. In addition such effects are also produced by application of DTT which may also stabilize closed conformation of the LBD.

We next evaluated single-channel properties on cysteine substituted N499C and Q686C in GluN1 (GluN1^c) and for K487C and N687C in GluN2A (GluN2A^c) mutants (Figure 4). There were significant differences in the mean shut time 5.62 ± 1.86 ms (119,858 events; $N=4$, $p<0.001$, one-way ANOVA) as compared to control. There was no significant difference in the mean shut times with GluN1^c / GluN2A^c mutant and UBP684 ($p=0.8724$). The open probability was increased with the GluN1^c / GluN2A^c mutant to 0.37 ± 0.062 ($p<0.001$) as compared to control. The open probability seen with UBP684, however was higher than the GluN1^c / GluN2A^c mutant ($p=0.0157$). There was no significant effect on

the mean open time with the GluN1^c / GluN2A^c mutant in comparison with that observed with control and in presence of UBP684. Next we compared the shut time constants and areas. As seen in figure 4 the overall shut time histogram in UBP684 resembles that by the locked-closed LBD mutant. Comparison of the shut times and areas suggest a close correlation between the effects of UBP684 and mutant.

F. Discussion

Here we have identified a novel NMDAR potentiator UBP684 which increases the peak response of GluN1/GluN2A and this effect is dependent on perforated or dialyzed mode of recording. The increase in deactivation kinetics by UBP684 suggest a possible increase in affinity for glutamate/glycine. Under steady state conditioning the increase in open probability by UBP684 can be accounted for by both an increase in the mean open time of the receptor and a reduction in the mean shut time.

Potentiation of GluN1/GluN2A NMDARs by UBP684 involves multiple time constants and multiple gating steps.

The rightward shift in the open time constants by UBP684 (Figure 3) as seen with the exponential fitting of the open time histograms suggest that the receptor UBP684 stabilizes the open state for longer duration. in both the short-lived and long-lived open states which might be a reason for the increase in mean open time. In addition to that, on fitting the shut time histograms with five exponential components, the peak seen with the control histograms (Figure 2) representing the long-lived shut time constants, is abolished

in presence of UBP684, greatly reducing the τ_2 and τ_3 long-lived shut-time constants, This is evident from the reduction in mean shut time observed with UBP684. The reductions in the τ_2 and τ_3 shut-time constants suggest a putative role of GluN2 subunit in the potentiation seen by UBP684 (Banke and Traynelis, 2003; Erreger et al., 2005). This could mean that the slower conformational change seen prior to channel opening is affected the most, reducing the peak seen with the conformational change of the GluN2 subunit.

Kinetic modeling was carried out using a model containing two open, three closed and two desensitized states. MIL fitting of single-channel data suggests that multiple gating steps were affected by the potentiation seen with UBP684. The slower gating steps were affected showing an increase the forward rate constants, driving the receptor faster into the open states. This is in accordance with the changes seen with shut-time constants t_2 and t_3 . The faster gating steps were also affected, keeping the receptor for a longer time in the open states, as seen with an increase in the open time constants t_1 and t_2 . The changes in slower rate constants represent a larger conformational change in the LBD of the GluN2 subunit. The faster rate constants represent that some gating mechanism near the pore of the ion-channel might be affected (Talukder and Wollmuth, 2011). The faster recovery from the desensitized states (D2-C2) implies that the receptor spends less time in long-lived desensitized state, which is also seen by the slower deactivation kinetics observed in dialyzed and perforated whole-cell recordings.

The potentiating effect of UBP684 can be better understood by studying the activity of NR1^c/NR2^c mutant.

For a better insight in understanding the effect of UBP684 single-channel recordings using the GluN1^c / GluN2A^c mutants were carried out. The LBD of the mutants were locked in a closed conformation, as they would behave if there was continuous presence of agonist bound in the cleft. Their shut-time histograms show similarity with the histogram seen with UBP684, wherein the long-lived shut time constants t_2 and t_3 are greatly reduced.

It has been suggested that even in the presence of saturating concentrations of agonists (here glutamate), the LBD domain undergoes fluctuations between opening and closing of the cleft. This might take place due to the unbinding and rebinding of agonists, and hence the peak seen with the GluN2B dependent shut-states is evident in the control shut-time histograms. Reductions in the peak with the mutants suggest that the LBD locked into a closed clamshell conformation increasing the efficacy of receptor into the open states (Kussius and Popescu, 2010). Similarly we can predict that UBP684 could be driving the receptor into more stable open states, and influencing the behavior of the receptor as if the LBD is continuously shut by the presence of a high efficacy agonist. The probable mechanisms by which UBP684 can cause this change is by acting somewhere on the LBD, preventing its closure, however not at the sites where orthosteric agents bind. It could also be acting near the pore of the ion-channel affecting the activation gate which is present on the M3 segment of the TMD.

Table 3: Time constants and areas of closed and open components obtained from exponential fits.

Comparison of the time constants (τ , in ms) and relative contribution (a, % area of the component) of the open time and shut time components obtained from individual fits to the cell-attached patches. Data are mean \pm SEM. The values were compared by unpaired *t*-test. *** indicates $p < 0.001$, ** indicates $p < 0.01$ and * indicates $p < 0.05$.

Time constants (ms) and areas (%)	0 Calcium			0.5 Calcium	
	Control (N=7)	UBP684 (N=9)	NR1c/NR2Ac (N=4)	Control (N=6)	UBP684 (N=5)
Open time					
τ_1	0.31 \pm 0.06	0.88 \pm 0.18*	0.73 \pm 0.19	0.57 \pm 0.10	0.64 \pm 0.09
τ_2	2.66 \pm 0.35	5.90 \pm 0.93*	2.40 \pm 0.25	2.33 \pm 0.30	1.79 \pm 0.21
a1	22 \pm 3	17 \pm 4	43 \pm 17	37 \pm 4	39 \pm 7
a2	78 \pm 3	83 \pm 4	56 \pm 17	63 \pm 4	61 \pm 7
Shut time					
τ_1	0.52 \pm 0.05	0.45 \pm 0.06	0.57 \pm 0.12	0.64 \pm 0.07	0.70 \pm 0.05
τ_2	4.37 \pm 0.93	1.66 \pm 0.24**	2.40 \pm 0.32	4.53 \pm 1.13	4.39 \pm 0.94
τ_3	15.9 \pm 2.8	5.73 \pm 0.9**	11.3 \pm 2.52	20.6 \pm 5.3	14.4 \pm 2.3
τ_4	49.4 \pm 9.7	65.1 \pm 45	70.2 \pm 13.2	69.1 \pm 21.8	121 \pm 60.4
τ_5	1375 \pm 370	1468 \pm 693	1060 \pm 314	1354 \pm 523	1386 \pm 307
a1	23 \pm 4	34 \pm 7	48 \pm 5	26 \pm 6	42 \pm 2*
a2	25 \pm 4	38 \pm 7	36 \pm 3	24 \pm 6	28 \pm 4
a3	40 \pm 4	23 \pm 4**	14 \pm 4	37 \pm 9	27 \pm 2
a4	11 \pm 2	4 \pm 1**	1.7 \pm 1	10 \pm 2	3 \pm 1*
a5	0.4 \pm 0.1	0.8 \pm 0.6	0.2 \pm 0.1	1.6 \pm 1.1	0.3 \pm 0.1

Table 4: Hidden Markov maximum interval likelihood fitting of the steady state currents.

Idealized current records were fitted to the gating scheme as described in Figure 7. All rates have units of s^{-1} . Data are mean \pm SEM from patches containing one active channel fitted individually. The rates were compared by unpaired *t*-test. *** indicates $p<0.001$, ** indicates $p<0.01$ and * indicates $p<0.05$.

Rates (s^{-1})	0 Calcium			0.5 Calcium	
	Control N=7	UBP684 N=9	NR1c/NR2Ac N=4	Control N=6	UBP684 N=5
$C_1 \rightarrow C_2$	165 \pm 35	315 \pm 35*	145 \pm 35	135 \pm 25	135 \pm 30
$C_2 \rightarrow C_1$	105 \pm 40	185 \pm 40	95 \pm 25	100 \pm 35	70 \pm 30
$C_2 \rightarrow C_3$	395 \pm 70	870 \pm 150*	505 \pm 85	320 \pm 80	290 \pm 70
$C_3 \rightarrow C_2$	1125 \pm 215	835 \pm 205	615 \pm 25	760 \pm 180	545 \pm 35
$C_3 \rightarrow O_1$	750 \pm 75	1325 \pm 110**	1345 \pm 200	780 \pm 120	865 \pm 70
$O_1 \rightarrow C_3$	1500 \pm 185	520 \pm 65***	1040 \pm 235	1135 \pm 250	1135 \pm 130
$O_1 \rightarrow O_2$	1890 \pm 465	710 \pm 235*	590 \pm 425	480 \pm 155	320 \pm 105
$O_2 \rightarrow O_1$	1155 \pm 170	690 \pm 100*	735 \pm 230	790 \pm 95	975 \pm 140
$C_1 \rightarrow D_1$	1.9 \pm 0.5	2.6 \pm 0.6	1.9 \pm 0.8	3.3 \pm 1.1	2.4 \pm 0.6
$D_1 \rightarrow C_1$	1.0 \pm 0.2	3.9 \pm 1.9	1.3 \pm 0.4	5.3 \pm 4.1	1.3 \pm 0.6
$C_2 \rightarrow D_2$	16.4 \pm 5.0	46.9 \pm 10*	9.7 \pm 4	23.6 \pm 10	8.0 \pm 2.9
$D_2 \rightarrow C_2$	30.5 \pm 7.1	40.5 \pm 10	15.9 \pm 2	35.4 \pm 7.9	19.7 \pm 6.1

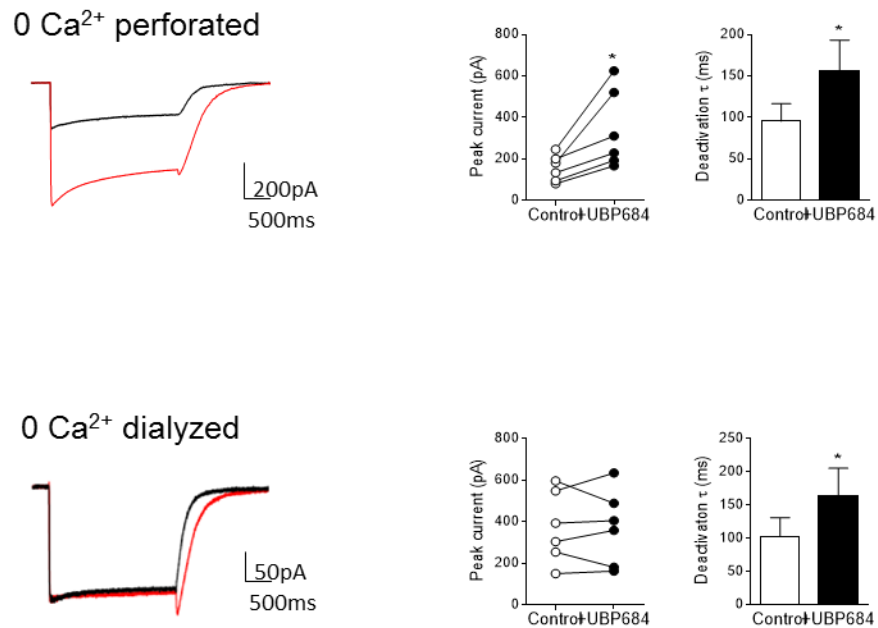


Fig. 1: Modulation of whole-cell responses by UBP684 is dependent on mode of recording

Whole-cell recordings under non-perforated (dialyzed) or perforated modes were obtained from HEK 293 expressing GluN1/GluN2A receptors (holding potential = -70 mV, filtered at 2 kHz, digitized at 5 kHz). Agonists (100 μ M glutamate and 100 μ M glycine) were applied in the absence (black traces) or presence of 100 μ M UBP684 (red traces) and the peak and steady state responses were evaluated. Responses were compared by paired *t*-test.

*

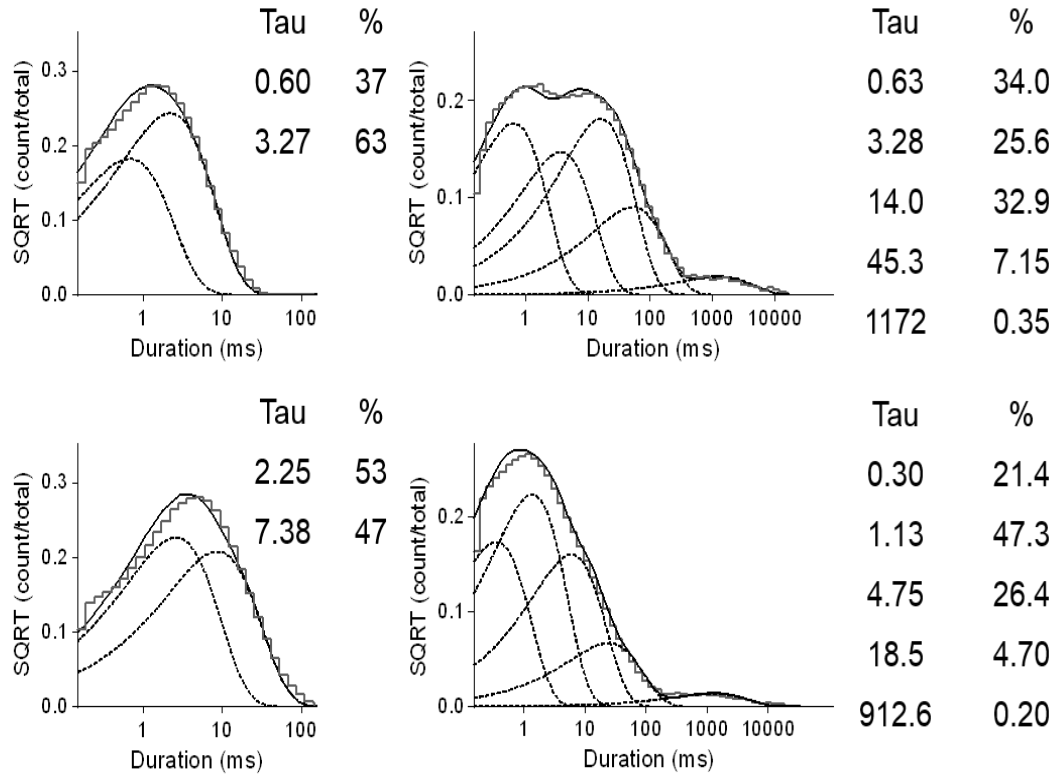


Fig. 2: UBP684 mediated potentiation of GluN1/GluN2A receptors involves a shift in open states to longer durations and a reduction in the occupancy of long-lived shut states.

The single-channel currents from cell-attached patches with one active GluN1/GluN2A receptor were idealized for each patch and summed to generate global dwell time histograms. The open time histogram was fitted by a sum of two exponential components: control, (n=7); UBP684 (n=7). The time constants and % area are shown in the inset. The dwell times from each patch were individually fitted and are presented in Table 1 The composite shut time histogram was fitted by a sum of five exponential functions: control, (n=7); UBP684 (n=7).

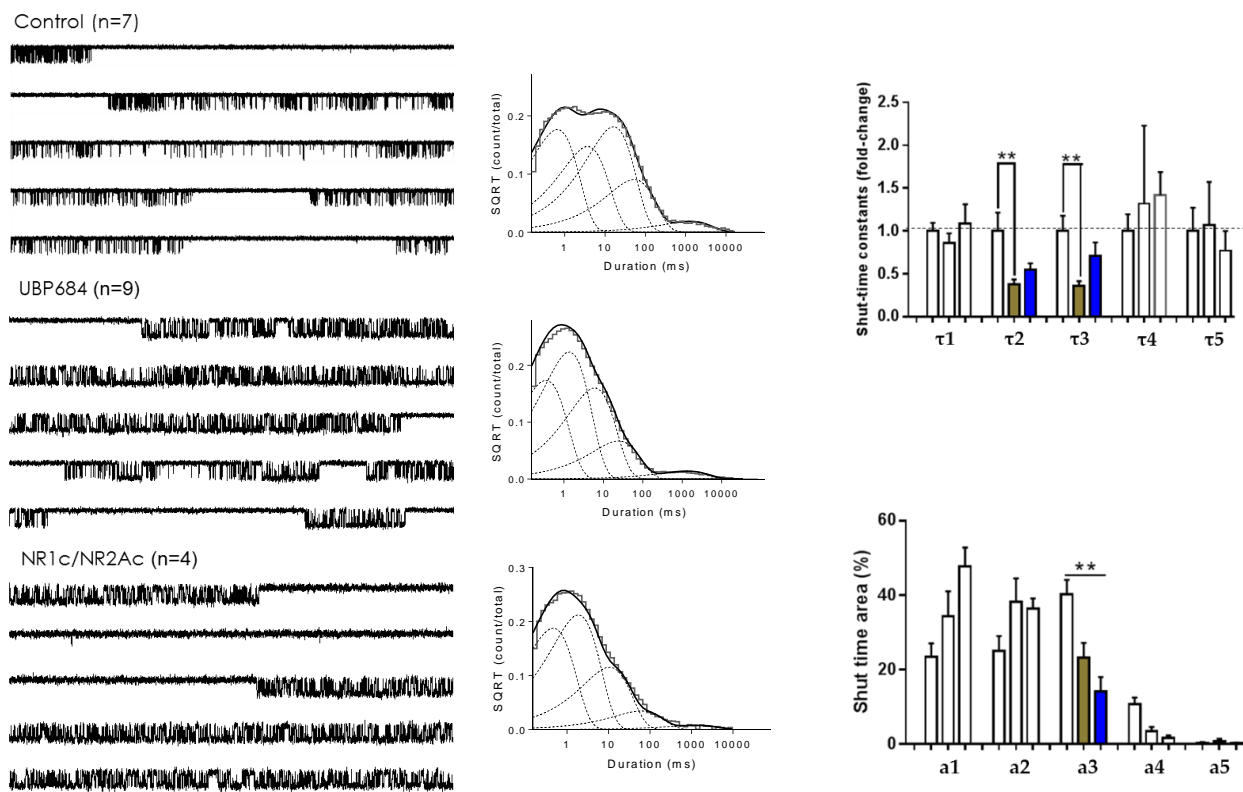


Fig. 3: Effect of UBP684 and NR1c/NR2Ac mutant on shut-time parameters

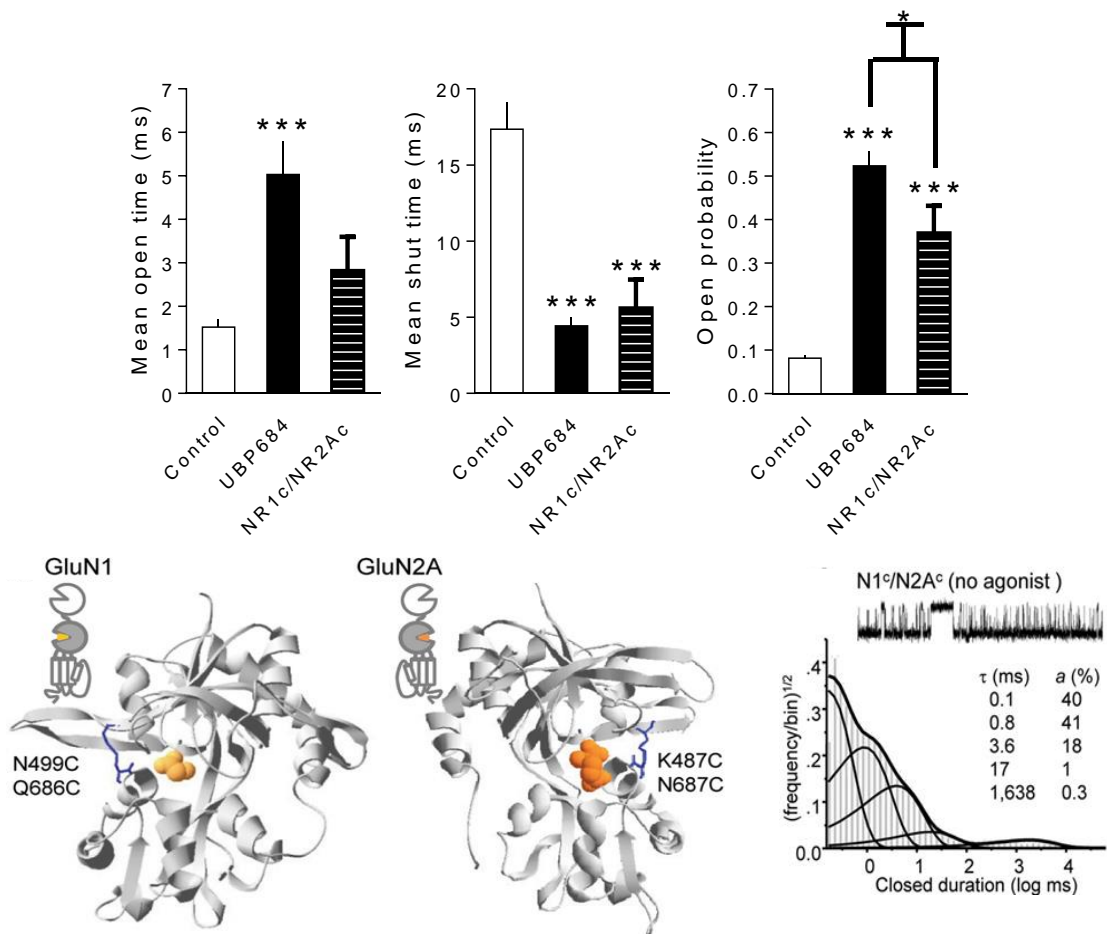


Fig. 4: Cysteine modifications in the LBD for obtained locked agonist binding clefts

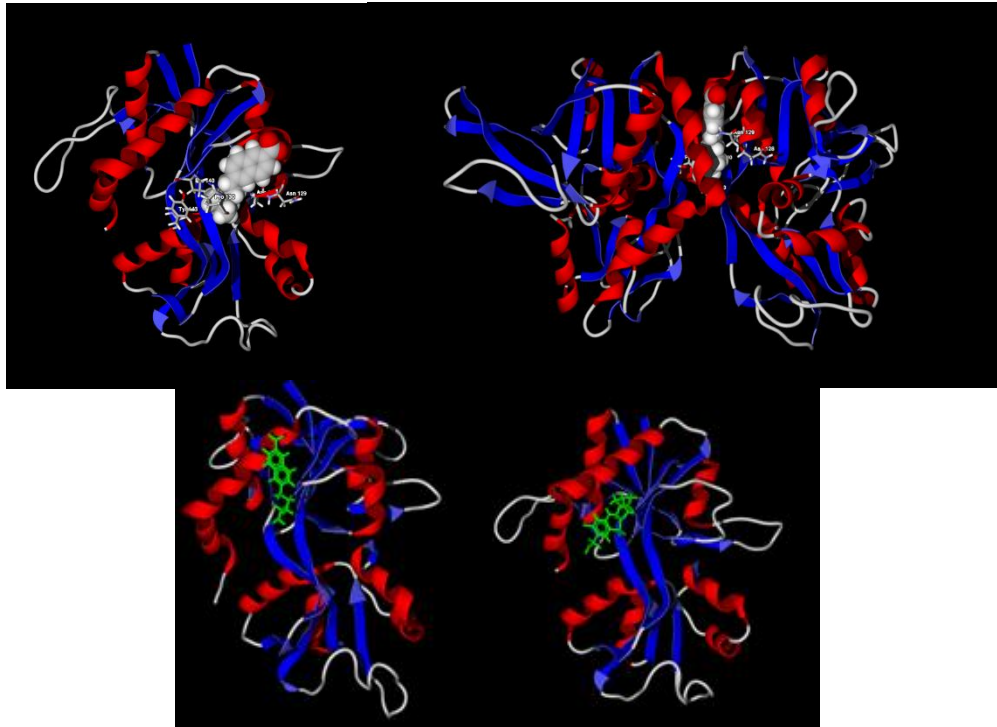


Fig. 5: Docking images which show the site of binding of UBP684 at GluN1/GluN2A receptors

G. References:

(Banke and Traynelis, 2003; Dravid *et al.*, 2007, 2008; Kussius and Popescu, 2010; Ogden and Traynelis, 2011; Talukder and Wollmuth, 2011; Bhatt *et al.*, 2013; Chopra *et al.*, 2015) Banke TG, and Traynelis SF (2003) Activation of NR1/NR2B NMDA receptors. *Nat Neurosci* **6**:144–52.

Bhatt JM, Prakash A, Suryavanshi PS, and Dravid SM (2013) Effect of ifenprodil on GluN1/GluN2B N-methyl-D-aspartate receptor gating. *Mol Pharmacol* **83**:9–21.

Chopra DA, Monaghan DT, and Dravid SM (2015) Bidirectional Effect of Pregnenolone Sulfate on GluN1/GluN2A NMDA Receptor Gating Depending on Extracellular Calcium and Intracellular Milieu. *Mol Pharmacol*, doi: 10.1124/mol.115.100396.

Dravid SM, Erreger K, Yuan H, Nicholson K, Le P, Lyuboslavsky P, Almonte A, Murray E, Mosely C, Barber J, French A, Balster R, Murray TF, and Traynelis SF (2007) Subunit-specific mechanisms and proton sensitivity of NMDA receptor channel block. *J Physiol* **581**:107–28.

Dravid SM, Prakash A, and Traynelis SF (2008) Activation of recombinant NR1/NR2C NMDA receptors. *J Physiol* **586**:4425–39.

Kussius CL, and Popescu GK (2010) NMDA receptors with locked glutamate-binding clefts open with high efficacy. *J Neurosci* **30**:12474–9.

Ogden KK, and Traynelis SF (2011) New advances in NMDA receptor pharmacology. *Trends Pharmacol Sci* **32**:726–33.

Talukder I, and Wollmuth LP (2011) Local constraints in either the GluN1 or GluN2 subunit equally impair NMDA receptor pore opening. *J Gen Physiol* **138**:179–94.

